



This is a repository copy of *Evidence for a novel Carbohydrate Binding Module (CBM) of Tannerella forsythia NanH sialidase, key to interactions at the host-pathogen interface.*

White Rose Research Online URL for this paper:  
<http://eprints.whiterose.ac.uk/128237/>

Version: Accepted Version

---

**Article:**

Frey, A.M., Satur, M.J., Phansopa, C. et al. (4 more authors) (2018) Evidence for a novel Carbohydrate Binding Module (CBM) of Tannerella forsythia NanH sialidase, key to interactions at the host-pathogen interface. *Biochemical Journal*, 475 (6). pp. 1159-1176. ISSN 0264-6021

<https://doi.org/10.1042/BCJ20170592>

---

© 2018 The Author(s). This is an author produced version of a paper subsequently published in *Biochemical Journal*. Uploaded in accordance with the publisher's self-archiving policy.

**Reuse**

Items deposited in White Rose Research Online are protected by copyright, with all rights reserved unless indicated otherwise. They may be downloaded and/or printed for private study, or other acts as permitted by national copyright laws. The publisher or other rights holders may allow further reproduction and re-use of the full text version. This is indicated by the licence information on the White Rose Research Online record for the item.

**Takedown**

If you consider content in White Rose Research Online to be in breach of UK law, please notify us by emailing [eprints@whiterose.ac.uk](mailto:eprints@whiterose.ac.uk) including the URL of the record and the reason for the withdrawal request.



[eprints@whiterose.ac.uk](mailto:eprints@whiterose.ac.uk)  
<https://eprints.whiterose.ac.uk/>

# Evidence for a Carbohydrate Binding Module (CBM) of *Tannerella forsythia* NanH sialidase, key to interactions at the host-pathogen interface

Frey, AM<sup>\*1</sup>, Satur, M.J. <sup>\*1</sup>, Phansopa, C<sup>\*1</sup>, Parker, JL<sup>1</sup>, Bradshaw, D., Pratten, J<sup>2</sup> & Stafford, GP<sup>†1</sup>

<sup>1</sup> School of Clinical Dentistry, The University of Sheffield, 19 Claremont Crescent, Sheffield, S10 2TA, UK

<sup>2</sup> Oral Health R&D, GlaxoSmithKline, St. Georges Avenue, Weybridge, KT13 0DE, UK

<sup>†</sup> author for correspondence

<sup>\*</sup> joint lead authors

## ABSTRACT

Bacterial sialidases cleave terminal sialic acid from a variety of host glycoproteins, and contribute to survival and growth of many human-dwelling bacterial species, including various pathogens. *Tannerella forsythia*, an oral, Gram-negative, fastidious anaerobe, is a key organism in periodontal disease, and possesses a dedicated sialic acid utilisation and scavenging (nan) operon, including NanH sialidase. Here, we describe biochemical characterisation of recombinant NanH, including its action on host-relevant sialoglycans such as sialyl Lewis A and sialyl Lewis X (SLe<sup>A/X</sup>), and on human cell-attached sialic acids directly, uncovering that it is a highly active broad specificity sialidase. Furthermore, the N-terminal domain of NanH was hypothesised and proven to be capable of binding to a range of sialoglycans and non-sialylated derivatives with  $K_d$  in the micromolar range, as determined by steady-state tryptophan fluorescence spectroscopy, but it has no catalytic activity in isolation from the active site. We consider this domain to represent the founding member of a novel subfamily of Carbohydrate Binding Module (CBM), involved in glycosidase-ligand binding. In addition, we created a catalytically inactive version of the NanH enzyme (FRIP→YMAP) that retained its ability to bind sialic acid-containing ligands and revealed for the first time that binding activity of a CBM is enhanced by association with the catalytic domain. Finally, we investigated the importance of Lewis-type sialoglycans on *T. forsythia*-host interactions, showing that nanomolar amounts of SLe<sup>A/X</sup> were capable of reducing invasion of oral epithelial cells by *T. forsythia* suggesting that these are key ligands for bacterial-cellular interactions during periodontal disease.

**KEYWORDS:** sialic acid, sialidase, lectins, oral microbiology, glycobiology

## **INTRODUCTION**

*Tannerella forsythia* is a Gram-negative anaerobic pathogen of the phylum Bacteroidetes, strongly associated with periodontal disease in humans [1]. Recent years have seen great strides forward in knowledge of the physiology and virulence factors of this previously under-studied organism [2], a fact that was mostly down to its fastidious growth requirements and requirement for inclusion of N-acetyl muramic acid (NAM) in growth media [3]. In particular, our group has shown that, at least in laboratory biofilm conditions, and possibly in vivo, NAM can be replaced by sialic acid as a growth factor for *T. forsythia* [4,5]. This ability to utilise sialic acid is dependent on a large sialic acid utilisation and harvesting locus [4,6,7], that are dedicated to the utilisation of free-monosaccharide sialic acid whereas in the human context sialic acid is found in a glyco-conjugated form attached most-often as the terminal moiety on N- or O-linked sialyl-glycoproteins or glycolipids, commonly known as sialoglycans [8]. Thus, unsurprisingly, bacteria have evolved the ability to release free-sialic acid from sialo-glycoproteins using surface-bound and secreted enzymes known as sialidases (or neuraminidases) that are capable of cleaving the  $\alpha 2,3$  or  $\alpha 2,6$  linkages that covalently attach sialic acid to underlying glycans [9–11]. Sialidases are a well conserved group of enzymes with well-studied examples including viral sialidases that are important for virulence, e.g. the neuraminidase of Influenza A viruses [12]. In the oral context, sialic acid is abundant in secretions such as saliva and the fluid located in sub-gingival environments, namely gingival crevicular fluid (GCF) [9]. Several groups of oral bacteria are known to produce sialidases, including several *Streptococcus* spp., *Actinomyces naeslundii*, *Capnocytophaga* spp., *Treponema denticola* and oral Bacteroidetes such as *Porphyromonas gingivalis* and *Tannerella forsythia* [9,13,14]. Their importance in virulence of periodontal pathogens is emerging, with mutants of *P. gingivalis*, *T. denticola* and *T. forsythia* that lack sialidases all being less virulent than their parent strains [13–15]. In addition it has now been shown that sialidase activity is raised in periodontal pockets in periodontitis and that high sialidase activity is indicative of poor prognosis to standard treatment, indicating its importance in clinical disease [16].

Recent work in our laboratory and others has revealed that *T. forsythia* produces a large sialidase enzyme (~57.4 kDa) with the ability to cleave sialic acid from the surface of human cells but also the model glycoprotein fetuin alongside more heterogeneous glycans contained within bovine submaxillary mucin and human saliva [15,17,18]. However, the exact nature of which

physiologically relevant epitopes it might target and detailed biochemical knowledge of its action are not known. In this paper, we have undertaken biochemical studies on the activity of this sialidase, characterised a novel Carbohydrate Binding Module (CBM), investigated its interactions with physiologically relevant ligands (Lewis-type), and identified the potential role of these ligands on interactions at the host-pathogen interface.

## METHODS

**Bacterial Cell Culture** — *Tannerella forsythia* strains ATCC 43037 and 92A.2 (gift from Floyd Dewhirst, Forsyth institute, Boston, USA) were grown on Fastidious Anaerobe Agar (FA; Lab M) supplemented with 5 % oxalated horse blood (Oxoid), 10 µg/mL NAM and 50 µg/mL gentamicin at 37 °C in an anaerobic cabinet with an atmosphere of 10 % CO<sub>2</sub>, 10 % H<sub>2</sub> and 80 % N<sub>2</sub>. Liquid cultures were grown in Tryptic Soy Broth (Oxoid) containing 0.4 % Yeast Extract, 10 µg/mL NAM, 50 µg/mL gentamicin, 5 µg/mL haemin and 1 mg/mL menadione. *Escherichia coli* strains were cultured in lysogeny broth (LB) at 37 °C with vigorous aeration, or on a solid LB medium containing 1.5 % bacteriological agar (Oxoid). Selective antibiotics were added to appropriate concentrations (e.g. 50 µg/mL ampicillin) prior to inoculation.

**Epithelial Cell Culture** — Cell culture and setup of invasion assays (below) was performed as previously described [19]. The oral squamous cell carcinoma (OSCC) cell line H357 was grown and maintained in T175 cm<sup>2</sup> tissue culture flasks (Greiner) at 37 °C in Dulbecco's Modified Eagle Medium (DMEM; Sigma-Aldrich) supplemented with 10 % (v/v) foetal bovine serum (FBS; Sigma-Aldrich) and 2 mM L-glutamine (Sigma-Aldrich) in an atmosphere containing 5 % CO<sub>2</sub>. Cells were grown under submerged conditions, trypsinised upon reaching 80 to 90 % confluence, counted using a haemocytometer and adjusted to 5 × 10<sup>3</sup> cells/mL and seeded into 24-well tissue culture plates (Greiner) with 1 mL of cell suspension per well, and left to grow for a further 48 h before cell adhesion/invasion assays were performed.

**Adhesion and Invasion Assay** — Assessment of the effect of exogenous ligands on host cell-*T. forsythia* association was performed using an adaptation of a previously described method [19]. Plate-cultured (5 days) *T. forsythia* ATCC 43037 were washed (3x) in Phosphate Buffered Saline (PBS; Sigma-Aldrich), counted in a Helber counting chamber and adjusted to 10<sup>7</sup> cells/mL. Semi-confluent H357 cell monolayers (at approximately 10<sup>5</sup> cells per well) were washed three times with PBS and incubated with bacteria at an MOI of 1:100 (5 % CO<sub>2</sub> at 37 °C) for 90 min. 0.22 µm Filter-sterilised solutions of Sialyl Lewis X (SLe<sup>X</sup>), Sialyl Lewis A (SLe<sup>A</sup>), Lewis X (Le<sup>X</sup>), Lewis A (Le<sup>A</sup>), 3'-sialyllactose (3-SL) and 6'-sialyllactose (6-SL) sodium salts (Carbosynth) and α-lactose monohydrate (Sigma-Aldrich) were added to a final concentration of 10 nM at the beginning of this incubation period. Non-adherent bacteria were then removed by washing with PBS (3x), and the total number of *T. forsythia* cells associated (invaded and adhered) with host cells was determined by osmotic cell lysis and plated by the Miles-Misra method (5 µL serial dilutions) in triplicate on

FA-NAM agar. To determine the number of invaded *T. forsythia*, cell surface-associated bacteria were killed by exposure to media containing 200 µg/mL metronidazole (1 h) before the cells were washed with PBS (3x), before internalised bacteria were released via osmotic shock and enumerated as before. The number of colonies of *T. forsythia* invaded and adhered (obtained by subtracting the total associated with the corresponding invaded count) were recorded and presented as means ± S.E.M., expressed as percentages of the number of viable bacterial count in the starting suspension which had been similarly exposed to the aerobic atmosphere and maintained in parallel with the invasion cultures. Statistical analysis was performed using one way ANOVA with Bonferroni correction for multiple comparisons, in Prism 7 (GraphPad Software), statistical significance inferred with a P-value of <0.05.

Cloning of the NanH Sialidases and Derivatives — The N-terminal region of BFO\_2207 (NanH, AEW22573.1) lacking the Sec-dependent secretion sequence (as predicted by SignalP 4.1 Server) was PCR amplified using Phusion high-fidelity DNA polymerase (New England Biolabs) from the genomic DNA of *T. forsythia* ATCC 43037 using primers BFO\_2207N-NdeI-F (5'-AATACATATGGCGGACAGTGTTTAC-3') and BFO\_2207N-XhoI-R (5'-AATACTCGAGCCCCATACGGCGCAC-3') to produce the carbohydrate-binding module (CBM; residues 33 to 197). The amplicon was inserted into the NdeI and XhoI sites of pET21a(+) expression plasmid (Merck Millipore), verified by sequencing and termed NanH-CBM in this manuscript (Core Genomic Facility, University of Sheffield). The entire open reading frame without the secretion sequence of *T. forsythia* nanH was synthesised (Eurofins) in an *E. coli* codon-optimised construct according to the sequence from the publically available genome sequence of *T. forsythia* 92A.2, which at the time was believed to be from strain 43037, but which was later identified as 92A.2 due to a misannotation (F. Dewhirst, Forsyth Institute, personal communication) such that changes in codon usage resulted in no changes in primary amino acid sequence. However, for the nanH gene, the mature 92A.2 and 43037 versions are 99% identical, excluding the signal sequence. Throughout the whole enzyme (539 amino acid residues) there are only eleven substitutions, of which none are within the FRIP motif or Asp-boxes (Supplementary figures S1 and S2). The gene was sub-cloned from the holding plasmid, pMA-RQ, into pET21a(+) using NdeI and XhoI as above, and its sequence was confirmed by DNA sequencing as above. Point mutants of nanH were produced using primers BFO\_2207-YMAP-F (5'-GCACCCGGATTAGTGACAACGAACAAAG-3') and BFO\_2207-YMAP-R (5'-CATATAAGAGGCTGATCCGTCGTC-3'), resulting in a change in the amino acid sequence from FRIP to YMAP in the active site region (aa 211–214) using the QuikChange Site-Directed Mutagenesis Kit (Stratagene) according to the manufacturer's instructions.

Production of Recombinant NanH, NanH Point Mutants and CBM Domains — *E. coli* BL21λ(DE3) was transformed with expression plasmids, grown as LB with 1 mM IPTG (isopropyl-β-D-thiogalactopyranoside) induction at OD<sub>600</sub> = 0.6, for 5 h at 37 °C with agitation. Cells were harvested and resuspended in 50 mM sodium phosphate, pH 7.4, 200 mM NaCl, 25 mM imidazole, disrupted using a French pressure cell at 1050 psi (2x), and soluble fractions clarified by further centrifugation (10,000 × g, 30 min, 4 °C). The C-terminally hexahistidine-tagged proteins were purified using a 1-mL HisTrap HP Ni<sup>2+</sup>-sepharose affinity chromatography column (GE Healthcare), and eluted with a 50 to 200 mM imidazole gradient on an ÄKTAprime plus (GE Healthcare). Purified proteins were dialysed against 50 mM sodium-potassium phosphate, pH 7.4, 200 mM NaCl, concentrated using a MWCO 10,000 Vivaspinn column (GE Healthcare) where necessary, and their concentrations determined using the Pierce BCA Protein Assay Kit (Thermo Scientific).

Ligand Binding Studies — The binding characteristics of purified NanH-CBM with candidate substrates were investigated by steady-state tryptophan fluorescence spectroscopy (the CBM possesses one tryptophan residue). Proteins were diluted in 50 mM sodium-potassium phosphate, pH 7.4, 200 mM NaCl, to a final concentration of 0.1 μM, from which 200 μL volumes were dispensed into the wells of an optically clear, flat-bottom 96-well plate (Greiner). Substrates at different concentrations were then pipetted into the wells and the microtitre plate was left to incubate at 25 °C for 10 min. The quenching of intrinsic tryptophan fluorescence was measured at 25 °C in a fluorescence spectrometer (Tecan M200) with the excitation wavelength set to 295 nm (5 nm slit-width) and emission spectra recorded over a scan range of 300–380 nm (10 nm slit-width). By monitoring the background fluorescence signal of NanH-YMAP or NanH-CBM to which no substrate was added, it was found that any downward drift was relatively minor when compared with the quenching of fluorescence signal due to a substrate-binding event. Corrections of fluorescence titration data were therefore not deemed to be necessary. Nonlinear regression and curve fitting of titration data were performed in Prism 7 (GraphPad Software), with the equilibrium dissociation constants (K<sub>d</sub>) for one site-specific binding calculated using Equation 1,

$$Y = B_{\max} \cdot X / (K_d + X) \quad (1)$$

in which X is the final concentration of ligand, Y is the percentage increase in protein quenching in relative to protein-only fluorescence signal, while B<sub>max</sub> is the extrapolated maximum specific binding.

pH Optima of *T. forsythia* Sialidase From Live Bacteria and of Purified NanH — Three-day cultures of *T. forsythia* were harvested from FA-NAM agar plates, resuspended in PBS, and washed twice by centrifugation at  $10000 \times g$  for 2 min and resuspended in PBS to  $OD_{600} = 1.0$ . *T. forsythia* suspension was added to the wells of a 96-well, clear, flat-bottomed plate (Greiner), and then diluted 1 in 20 in buffers of variable pH containing 20 mM of either sodium citrate-citric acid (pH 3.0–6.4), sodium phosphate monobasic-dibasic (pH 6.8–8.8), or sodium carbonate-sodium bicarbonate (pH 9.2–10.5) (buffers prepared according to instructions supplied by Sigma Aldrich). Buffers also contained 0.1 mM 4-methylumbelliferyl N-acetyl neuraminic acid (MU-NANA; Carbosynth), which results in the liberation of methylumbelliferone (4-MU) from MU-NANA. *T. forsythia*-MU-NANA reactions were incubated at 37 °C and stopped at 30 min intervals by quenching the reaction in 100 mM sodium carbonate-sodium bicarbonate buffer, pH 10.5, with a volume ratio of 1:1.5. This also equilibrated the pH in all reactions and enabled maximum fluorescence of 4-MU during quantification. A microplate reader (Tecan Infinite M200, Tecan), was used to quantify sialidase activity by measuring 4-MU fluorescence ( $\lambda_{ex} = 350$  nm;  $\lambda_{em} = 450$  nm). To assay purified NanH, reactions were performed as described for live bacteria, but NanH was present in reactions at 2.5 nM, and reactions were quenched by the addition of the described sodium carbonate buffer every 30 s.

Reaction Kinetics of Purified NanH and MU-NANA — Reaction kinetics of NanH under pH optimum and physiological mimicking conditions were obtained: 2.5 nM NanH was incubated in the presence of a variable concentration of MU-NANA (0–200  $\mu$ M), in one of four different buffers appropriate to their pH buffering ranges (20 mM sodium citrate-citric acid, pH 5.6, or 20 mM sodium citrate-citric acid with 200 mM NaCl, pH 5.6, or 20 mM sodium phosphate monobasic-dibasic pH 7.4, or 50 mM sodium phosphate monobasic-dibasic, with 200mM NaCl, pH 7.4). Reactions were quenched by the addition of 100 mM sodium carbonate buffer, pH 10.5, every 30 s at a volume ratio of 1:1.5 (reaction: sodium carbonate), and sialidase activity quantified by measuring 4-MU fluorescence ( $\lambda_{ex} = 350$  nm;  $\lambda_{em} = 450$  nm). Against a standard curve of the fluorescence signal of 4-MU at defined concentrations, sialidase activity was expressed as 4-MU released,  $\mu$ mol/min/mg NanH.

Nonlinear regression and curve fitting of the time course data (4-MU release by NanH) were performed in Prism 7 (GraphPad Software) to obtain the maximal enzyme velocity ( $V_{max}$ ) and Michaelis–Menten constants ( $K_M$ ), as calculated using Equation 2,

$$v_0 = V_{\max} \cdot [S] / (K_M + [S]) \quad (2)$$

$$v_0 = k_{\text{cat}} \cdot [E_t] \cdot [S] / (K_M + [S]) \quad (3)$$

in which  $v$  is the reaction rate,  $[S]$  is the concentration of substrate MU-NANA, plotted as initial velocity ( $v_0$ ), at a specific  $[S]$  on the Y- and X-axes, respectively. Substrate turnover,  $k_{\text{cat}}$ , was calculated from the concentration of enzyme site ( $E_t$ ) as shown in Equation 3.

Reaction Kinetics of Purified NanH and Host-Relevant Ligands — To obtain the glycosidic linkage preference of NanH for  $\alpha$ 2-3- or  $\alpha$ 2-6-linked sialic acid, and preference for SLe<sup>A</sup> or SLe<sup>X</sup> under physiological-mimicking conditions, 50 nM NanH was incubated in the presence of variable concentrations of 3-SL, 6-SL, SLe<sup>A</sup> or SLe<sup>X</sup> (Carbosynth) in 50 mM sodium phosphate monobasic-dibasic buffer, 200 mM NaCl, pH 7.4, for up to **10 min** at 37 °C. Reactions were halted by the addition of 25  $\mu$ L sodium periodate to 50  $\mu$ L reaction mixture. This commenced the first step of a modified version of the thiobarbituric acid (TBA) assay, for assessment of free sialic acid [20,21]. 50  $\mu$ L of these reactions containing sialic acid were added to 25  $\mu$ L of 25 mM sodium periodate (Sigma Aldrich) in 60 mM H<sub>2</sub>SO<sub>4</sub> (Thermo Fisher) and incubated for 30 min at 37 °C. This oxidation step was stopped by the addition of 20  $\mu$ l of 2 % (<sup>w/v</sup>) sodium meta-arsenite (Sigma Aldrich) in 500 mM HCl. 47  $\mu$ L of this reaction was added to 100  $\mu$ l of 100 mM TBA, pH 9.0, and incubated at 95 °C for 7.5 min, resulting in the thiol-labelling of free sialic acid. Upon centrifugation at 1500  $\times$  g for 5 min, the pink chromophore in the clarified supernatant was spectrophotometrically quantified at A<sub>549</sub>. A standard curve of known sialic acid (Neu5Ac, Carbosynth) concentrations was used to calculate sialic acid release in  $\mu$ mol/min/mg NanH. After plotting sialic acid release under different concentrations of substrates (3-SL, 6-SL, SLe<sup>A</sup> and SLe<sup>X</sup>), the kinetic parameters  $K_M$ ,  $k_{\text{cat}}$  and  $V_{\max}$  were determined as above for MU-NANA, using Equations 2 and 3.

Sialidase Treatment, 3- and 6-Linked Sialic Acid and Sialyl Lewis Staining — H357 cells were passaged as described, seeded onto glass coverslips, one per well in a 24-well tissue culture plate (Greiner,  $1 \times 10^5$  cells/well). Cells were incubated overnight at 37 °C in 5 % CO<sub>2</sub>. Adhered cells were washed twice in PBS, and incubated in 50mM sodium phosphate monobasic-dibasic, 200 mM NaCl, pH 7.4, with or without 200 nM NanH at 37 °C in 5 % CO<sub>2</sub> for 2 h. Treated cells were then washed twice in PBS and fixed by incubation in 2 % paraformaldehyde at 4 °C for 16–18 h or 37 °C for 15 min. Fixed cells were stained for SLe<sup>X</sup> or SLe<sup>A</sup> by incubation with 0.2  $\mu$ g/mL anti-SLe<sup>X</sup> IgM or 2  $\mu$ g/mL anti-SLe<sup>A</sup> IgG<sub>1</sub> mouse monoclonal antibodies (Merck Millipore), respectively, at 37 °C for 45 min. Negative isotype controls were generated by incubating PBS-

treated cells with 2  $\mu\text{g}/\text{mL}$  mouse anti-rat IgM (Sigma-Aldrich) or 0.2  $\mu\text{g}/\text{mL}$  mouse anti-rat IgG<sub>1</sub> (Bio-Rad) and incubated as above. SLe<sup>X</sup>, SLe<sup>A</sup> and isotype stained cells were washed twice with PBS and incubated with 4  $\mu\text{g}/\text{mL}$  goat anti-mouse Alexa Fluor 488 dye (Life Technologies) at 37 °C for 45 min. Coverslips with stained cells were mounted onto glass microscope slides using ProLong Gold antifade reagent with DAPI (Life Technologies). For 3- and 6-linked sialic acid staining, NanH-treated cells were stained with lectins from Sambucus nigra (SNA) and Maackia amurensis (MAA). Cells were incubated with 4  $\mu\text{g}/\text{mL}$  SNA-fluorescein isothiocyanate conjugate (SNA-FITC; Vector Labs) or 8  $\mu\text{g}/\text{mL}$  biotinylated-MAA (Vector Labs), for 30 min at 37 °C with 5% CO<sub>2</sub>. Cells were washed twice with 500  $\mu\text{L}$  PBS and in conditions containing biotinylated lectin, underwent a second incubation with 2  $\mu\text{g}/\text{mL}$  Texas Red-Streptavidin, for 30 min at 37 °C. Lectin-stained cells were washed three times with 500  $\mu\text{L}$  PBS and fixed with 500  $\mu\text{L}$  2% (w/v) paraformaldehyde (PFA) for 15 min at 37 °C.

Visualisation and Quantification of SLe<sup>X</sup> and SLe<sup>A</sup> — After mounting, cells were visualised using an Axiovert 200 fluorescence microscope (Zeiss) and AxioVision image analysis software (version 4.6; Zeiss) under 400  $\times$  magnification using blue (DAPI) and green (Alexa Fluor 488) channels. Fluorescence intensity and exposure time for each image was set manually, and remained constant during for all conditions during each experiment. Fiji image analysis software [22] was used to process all images, with processing parameters (i.e. background fluorescence subtraction) kept constant between all images. In addition to visual examination, the level of SLe<sup>X</sup> or SLe<sup>A</sup> in each condition was quantified using the mean pixel intensity of the green channel, normalised to cell number, in three fields of view, in three separate experiments, and expressed as the mean fluorescence  $\pm$  S.E.M.

## RESULTS AND DISCUSSION

### **NanH is a highly active sialidase with broad pH activity**

Sialidases are a phylogenetically broadly distributed group of enzymes that have highly conserved catalytic domains with a characteristic 5–6-blade  $\beta$ -propeller structure and are classified as GH33 Glycosyl Hydrolase Carbohydrate Active Enzymes [23–25]. The sialidase from *T. forsythia* contains typical sialidase conserved primary sequence motifs, such as the five Asp-boxes (with the sequence Ser/Thr-X-Asp-X-Gly-X-Thr-Trp/Phe, where X represents any amino acid) that are evenly spaced throughout the sialidase structure, the F/YRIP motif and a conserved catalytic arginine triad that often co-ordinates the carboxylate group of sialic acid (Supplementary figures S1 and S2, [24,26]). Alignment of the *T. forsythia* NanH amino acid sequence reveals that its closest

homologues are putative sialidases from *Parabacteroides distasonis* (74 % identical), *Parabacteroides gordonii* (75 % identical) and *Bacteroides fragilis* (66 % identical).

Typically, bacterial sialidases function with an acidic pH optimum of around pH 5–6, and a previous study which expressed the *T. forsythia* NanH in *E. coli* and analysed its biochemical activity from *E. coli* cell lysates only observed a pH optimum of pH 5.5 [18]. However, in order to more thoroughly examine the biochemical properties of this enzyme we cloned and expressed a codon-optimised version of the *T. forsythia* NanH sialidase in *E. coli*, with a C-terminal hexahistidine-tag. In contrast to previously produced native *T. forsythia* gene sequence based clones [15,17], we were able to produce the enzyme at high levels in a soluble form without the need for complex purification protocols and purified it to high homogeneity (Supplementary figure. S3). In order to determine the activity and specificity profile of this purified recombinant version of NanH, we performed activity assays using the MU-NANA substrate across a range of pH values, showing that NanH has optimal activity at around pH 5.2–5.6 and is active across a wide range of pH values (Figure 1A), still being ~30 % of maximal activity at pH 7.6.

In addition, we assessed the activity of this enzyme in its native context, i.e. in assays using two strains of *T. forsythia* (ATCC 43037 and 92A.2) in whole cell assays. These were performed in the manner described for purified NanH, except that standardised amounts of bacterial cells were used in place of purified enzyme, and revealed largely similar trends to the NanH data except that the pH optimum was slightly higher, and the activity profile even broader with ~30–40 % of activity maintained even at pH 8 (Figures 1B and 1C).

These findings fit well in the context of the subgingival biofilm niche that *T. forsythia* chiefly inhabits, where studies have detected a link between inflammation and pH of the GCF, i.e. a basic pH was associated with periodontitis progression [27]. However, others have failed to find this association [28], or that there are wide variations in pH even within a single periodontal pocket [29]. Differing pH is also seen in the supra-gingival environment, where pH has been shown to vary widely in short spaces of time and space, i.e. after food consumption [30], in laboratory studies of individual organisms [31], and mixed species oral biofilms [32,33]. Ultimately, it is likely that the ability of sialidase to function under a wide variety of pH conditions would enable *T. forsythia* to more effectively colonise the sub- and supra-gingival plaque biofilms, further supporting our hypothesis that it is highly active in the environmental conditions in which it resides. While the biochemical basis of this phenomenon is unknown it is possible that surface association of NanH on whole bacteria alters the conformation and the local environment of the protein and thus its pH

optimum. It is also of note that both the *T. forsythia* strains 92A.2 and ATCC 43037 displayed this trend for activity over broad pH ranges, indicating it is not just restricted to the type strain. In addition, several periodontal species have an optimum for growth at neutral-basic pH ranges [34,35], while several other secreted virulence factors, such as the gingipains of *P. gingivalis* and the secreted matrix metalloprotease (MMP) karilysin and NanS sialate-O-acetyltransferase from *T. forsythia* have pH optima around pH 7–8 [36–38].

### **Biochemical study of NanH reveals a broad substrate and linkage preference range**

Once we had established the optimal pH for activity, we utilised the same umbelliferyl substrate to establish the Michaelis–Menten kinetics of this enzyme under its optimum acidic pH (pH 5.6), physiological (pH 7.4), and physiological-salt-mimicking conditions, i.e. with 200 mM NaCl (Figure 2). The affinity ( $K_M$ ) of NanH for MU-NANA at the optimum pH 5.6 condition used in this study was determined to be  $21.37 \pm 1.24 \mu\text{M}$ , a similar finding to that described by Thompson et al. [18], who determined the  $K_M$  from whole crude lysates of *E. coli* to be  $32.9 \pm 10.3 \mu\text{M}$  (the  $V_{\text{max}}$  is not comparable since Thompson et al. performed experiments using cell lysates while we used pure protein). Notably the  $K_M$  was lower at pH 7.4 ( $13.8 \pm 2.152$ ) but the enzyme efficiency was over 2-fold higher at pH 5.6. However, the presence of NaCl did not significantly affect affinity or the catalytic efficiency ( $k_{\text{cat}}/K_M$ ) of NanH at either pH, i.e. was 55.21 and 48.73  $\mu\text{M}/\text{min}$  at pH 7.4, and 130.1 to 126.68  $\mu\text{M}/\text{min}$  at pH 5.6 (Figure 2 B), a surprising observation given that 200mM NaCl is mimicks physiological salt concentrations in the body,

While the MU-NANA substrate allowed basic biochemical characterisation of NanH, in order to test its activity with more relevant host-like glycans that are likely targeted by NanH at the host-pathogen interface, we employed a modified version of the thiobarbituric acid (TBA) assay to measure the amount of sialic acid released from more complex sialyl-glycans [20,21]. In this work, we focused on examining its preference for  $\alpha$ 2,3- or  $\alpha$ 2,6-linked sialic acid using 3-SL and 6-SL trisaccharides, and SLe<sup>A</sup> and SLe<sup>X</sup> (Supplementary figure S4) which are known to be present on epithelial cell surfaces and in salivary and membrane mucins [39,40]. Colominic acid was also exposed to NanH and TBA assays performed to assess cleavage of  $\alpha$ 2-8 polysialic acid (present on neuronal cell surfaces), and in this case we detected no sialic acid release (data not shown). This is comparable to previous studies where lysates of *E. coli* expressing NanH showed no  $\alpha$ 2-8 polysialic acid cleavage [18].

Kinetic studies of  $\alpha$ 2-3 and  $\alpha$ 2-6-linked sialic acid using the trisaccharides 3-SL and 6-SL revealed that NanH is capable of cleaving 3- and 6- linked sialic acid under physiological-mimicking

conditions, with a preference for the  $\alpha$ 2-3 epitope (Figures 3 A and C,  $K_M = 0.31 \pm 0.03$  and  $0.60 \pm 0.07$  mM,  $V_{max} = 46.44 \pm 1.21$  and  $31.56 \pm 0.96$  for 3-SL and 6-SL, respectively). A finding that was reflected by the catalytic efficiencies, with NanH displaying almost threefold greater efficiency in sialic acid release from 3-SL (Figure 3 C,  $k_{cat}/K_M = 8655$  mM/min and  $3038$  mM/min for 3-SL and 6-SL, respectively). This ability to act on both  $\alpha$ 2-3- and  $\alpha$ 2-6-linked sialic acid is shared by the majority of bacterial sialidases present in human mucosal organisms, although many do display a preference for one of the two linkages, with  $\alpha$ 2-3 more commonly observed as a specificity preference (Table 1). In the context of oral bacterial sialidases knowledge of linkage preference is limited, but those that have been characterised display slightly greater activity on  $\alpha$ 2-3-linked sialic acid which may make sense given high levels of  $\alpha$ 2-3 sugar in salivary mucins (Table 1).

The activity of NanH against SLe<sup>A</sup> and SLe<sup>X</sup> was also assessed (Figure 3B and C). Both possess  $\alpha$ 2-3-linked sialic acid, but different linkages between their other constituent sugars (supplementary Figure S4). NanH displayed similar affinity and  $V_{max}$  for the two epitopes ( $K_M = 1.26 \pm 0.24$  and  $1.07 \pm 0.21$  mM,  $V_{max} = 36.11 \pm 2.59$  and  $31.24 \pm 2.13$   $\mu$ mol/min/mg NanH for SLe<sup>A</sup> and SLe<sup>X</sup>, respectively), and the catalytic efficiency of NanH for the two ligands was also similar ( $k_{cat}/K_M = 1645$  and  $1675$  mM/min for SLeA and SLeX, respectively). Notably, the catalytic efficiency of NanH for the sialyl Lewis ligands was over fourfold less than for 3-SL, despite all three possessing  $\alpha$ 2-3 linked sialic acid. This highlights the importance of underlying glycan moieties in sialidase activity. While it is difficult to establish Michaelis-Menten kinetics using larger sialoglycans or mixed oligosaccharide solutions, NanH has been shown to cleave sialic acid from bovine submaxillary mucin and fetuin [38] (containing a variety of mucins representing a complex mixture of sialoglycoproteins) and here we show NanH to be capable of cleaving sialic acid from oral cell surfaces (Figure 7, supplementary figure S7, discussed below), in line with previous studies [15]. In addition to glycan structure impacting enzyme-substrate interactions, our ongoing unpublished experiments suggest the formation of dimers and tetramers by NanH in solution (data not shown), which may act to increase NanH-ligand avidity. Furthermore, in addition to secreted-extracellular NanH, there is evidence that NanH can be localized to the bacterial cell surface [15], and clustering of NanH could also occur in this location, further improving avidity. Indeed, differences in clustering between soluble and membrane-associated NanH could explain the variation in NanH activity under different pH conditions (discussed above). Studies with immunogold labelling could be used to investigate clustering of NanH at the surface of *T. forsythia*, but at present we do not have access to antibodies required for such experiments.

### **The NanH sialidase putative CBM is a broad specificity lectin domain**

While the catalytic domains of bacterial sialidases are relatively well-conserved, with signature motifs, these catalytic domains are often preceded, followed or flanked in the protein structure (and sequence) by domains that may help align the target glycoconjugates via the use of lectin-like domains or carbohydrate binding modules (CBM). One well-known example being that of the sialidase of *Vibrio cholerae* which contains two lectin-like domains (classified as CBM40) that appear to co-ordinate its cellular ligands [23,41]. A similar situation might exist in the case of the *T. forsythia* NanH sialidase, where a ~160 aa N-terminal extension exists, which homology searches [9] and structural predictions (not shown) show to be distinct from the predicted catalytic  $\beta$ -propeller domain. However, BLAST and Pfam database searches of this 'N-terminal domain' do not reveal any homology with other documented lectin domains or CBM modules documented in the CAZy database [25]. We aligned the mature N-terminal domains of several (putative) sialidases from three *T. forsythia* strains and other closely related Bacteroidetes (Figure 4). This revealed significant homology between sialidases from *T. forsythia*, *Bacteroides* and *Parabacteroides* spp. and indicated that this domain is conserved amongst sialidase from this group of bacteria. Given the incidence of homologues of this domain in a range of predicted sialidases, we hypothesised that it might bind relevant sialyl-conjugate sugars with high affinity. In order to establish this the N-terminal amino acid residues 33-197 of NanH were amplified and cloned from the *T. forsythia* genome by PCR, ligated into pET21a(+) plasmid vector, expressed recombinantly and purified to homogeneity as an 18-kDa protein (Supplementary figure S5). The NanH-CBM is a highly soluble domain, with no sialidase activity (as tested using MU-NANA, not shown).

In order to test whether the NanH-CBM is a novel lectin domain protein we performed steady-state tryptophan quenching ligand binding experiments on purified NanH-CBM (Figure 5). NanH-CBM has no apparent affinity for the monomeric form of sialic acid Neu5Ac (or di-O-acetylated Neu5,9Ac, not shown). However, it is capable of binding various oligosaccharide glycans in their sialylated and non-sialylated forms with  $K_d$  in the  $\mu$ M range, indicating that it is a broad specificity CBM. In addition to binding both sialylated and non-sialylated glycans, the finding that NanH-CBM does not bind monomeric sialic acid (Neu5Ac or Neu5,9Ac) is in contrast to previously characterised CBMs from other bacterial sialidases from *V. cholerae* [41], *Streptococcus pneumoniae* [42,43], and *Clostridium perfringens* [44] and represents a clear affinity for oligosaccharide glycoconjugates, possibly representing its role in docking to and orientation into the active site of a broad range of human glycoconjugates that it might encounter in vivo. We therefore believe that the *T. forsythia* NanH-CBM represents the founding member of a novel CBM family, distinct from those of previously characterised bacterial sialidases.

### **Mutation of the FRIP domain of NanH abolishes catalytic but not binding activity**

In this study, we sought to completely abrogate NanH sialidase activity by mutating the FRIP motif in order to more fully characterise and probe the activity of *T. forsythia* NanH and its binding to sialylconjugate ligands in the absence of catalytic turnover. To achieve this, we produced a version with the FRIP residues mutated to YMAP (NanH-YMAP), which we consider a conservative mutation strategy given that Y often substitutes for F in this motif in other sialidases while methionine (M) is closer in predicted space-fill to the arginine (R) residue that normally occupies this position, and finally that alanine (A) was considered an appropriate substitution for I, since these two amino acids are similar in mass and hydrophobicity. These substitutions resulted in production of a version of NanH-TF that had no residual sialidase activity when incubated with MU-NANA (Supplementary figure. S6B), while still producing a highly soluble protein at high levels in *E. coli* (Supplementary figure S6A). In addition, our group has recently obtained a preliminary crystal structure of both NanH-TF and NanH-YMAP, and there are no broad structural changes resulting from this substitution (not shown, manuscript in preparation).

To test whether this mutant still bound ligand successfully (a proxy indicator of folding) and that the inactivity was due solely to the mutation made and not an inability to co-ordinate or bind ligand, we again tested binding via a tryptophan quenching strategy. As shown in Figure 6, NanH-YMAP still binds 3-SL and 6-SL, with higher affinity (lower  $K_d$ ) for 3-SL than 6-SL, a trend implied from the  $K_M$  data for NanH (albeit representing substrate turnover rather than ligand binding per se). We acknowledge that this data does not discriminate between binding at the active site or in the putative CBM, however, we do not observe sigmoidal binding or activity curves, while the Hill equation does not indicate any evidence for cooperativity (not shown). When we performed binding experiments with wild-type NanH (Fig. S8) we saw similarly higher affinity binding with the full protein ( $K_d$  for 3-SL (152 mM) and 6-SL (418 mM)) than the CBM, although the data are harder to interpret given the mixture of cleaved and uncleaved ligand likely to be present in experiments with active enzyme, especially in the case of 6-SL where turnover is lower. One outcome of this experiment is that we see 2-fold higher affinity in binding experiments for 3-SL and 6-SL for the YMAP mutant (and wild-type enzyme) than the CBM alone, suggesting that the alignment of the CBM within the mature enzyme increases its avidity for oligosaccharide ligands. These experiments build on previous work highlighting the importance of the F/YRIP motif in catalytic function of the *Clostridium perfringens* sialidase [45], where arginine was mutated to isoleucine, resulting in reduction in enzyme activity with 3-SL by tenfold. Overall we have not only confirmed the role of the FRIP motif in NanH catalysis, but also revealed that the binding activity of the CBM is

enhanced by its association with its cognate catalytic domain.

### **NanH targets Sialyl Lewis antigens on the surface of oral epithelial cells**

In previous work we had illustrated the ability of NanH to release sialic acid from fetuin [17], while Honma et al. [15], illustrated cleavage of  $\alpha$ 2,3-linked sialic acid from the surface of gingival epithelial cells. In order to further characterise this enzyme activity, we re-confirmed this cleavage of  $\alpha$ 2,3-sialic acid from epithelial cells but also  $\alpha$ 2,6-linked sialic acid as detected with SNA and MAA lectins (Supplementary figure S7). However, to further investigate the previously unobserved activity against SLe antigens, we used SLe<sup>A</sup>- and SLe<sup>X</sup>-specific antibodies to probe the ability of NanH to act on these antigens in their native context, i.e. on oral epithelial cell surfaces.

These experiments revealed that NanH was able to reduce levels of SLe<sup>A</sup> and SLe<sup>X</sup> at the surface of oral epithelial cells, both by qualitative observation but also by quantifying fluorescence of cells treated with NanH, in three separate experiments (Figure 7). In these experiments, NanH reduced staining of cell surface SLe<sup>A</sup> and SLe<sup>X</sup> from 3.51 to 1.17 MFI/cell ( $P = 0.008$ ), and 3.26 to 1.03 MFI/cell ( $P = 0.002$ ). Thus, in addition to highlighting NanH targeting of  $\alpha$ 2,3- and  $\alpha$ 2,6-linked sialic acid on the surface of oral epithelial cells, we have also set this ability in the context of larger glycan structures that might be targeted by this enzyme — and *T. forsythia* itself — during its interactions with human cells in the oral cavity. These experiments extend the observations of CBM binding and enzyme kinetics by proving that NanH acts upon complex human cell surface glycans and build upon our previous work showing cleavage of salivary glycans [17].

### **Exogenous Lewis Sugars Influence *T. forsythia* interactions with human cells**

Since we had shown both an interaction of the CBM with Lewis antigens and the ability of NanH to cleave sialic acid from the surface of epithelial cell bound SLe<sup>A/X</sup>, we now aimed to investigate whether SLe antigens were a potential in vivo ligand for *T. forsythia* during infections. To achieve this, we set up monolayer epithelial cell interaction studies where the oral epithelial cell line H357- previously established as a model for bacteria-host cell association [19,46], was challenged with live *T. forsythia* in the presence and absence of sialylated- and non-sialylated-Lewis antigens (all at 10 nM). We observed a striking reduction in association, attachment, and invasion of *T. forsythia* during infection of oral epithelial cells in the presence of these ligands (Figure 8). The most striking reduction was seen for invasion, where the proportion of *T. forsythia* invading the oral epithelial cells was 0.84 % in the absence of Lewis ligand, and was reduced by Le<sup>X</sup>, SLe<sup>X</sup>, Le<sup>A</sup> and SLe<sup>A</sup> to 0.54 %, 0.15 %, 0.77 %, and 0.22 % ( $P = 0.0001, 0.0001, 0.2, \text{ and } 0.0001$ ), respectively, with the sialylated versions having the greatest impact. Importantly, the total number

of associated (the sum of both attached and invaded) bacteria was consistently reduced in the presence of all ligands tested, and again, the sialylated versions had the greatest impact. Perhaps, surprisingly, the amount of attached bacteria (indicating adherence) was not so clearly affected; however, this is more difficult to interpret given that strong interaction may well result in internalisation of bacteria whereas weakly or non-productive interactions may result in bacteria remaining surface associated but not internalised. Between the two sialylated-Lewis ligands, SLe<sup>X</sup> is perhaps the most well studied isomer, known for its role in neutrophil migration, where it is expressed on the surface of neutrophils and binds E-selectin present on endothelial cells, enabling crawling motility and neutrophil migration across the endothelium into target tissues [47]. However, the role of E-selectin in this particular interaction is unlikely given its predominantly endothelial localisation and given that knowledge of its expression on normal epithelial cells is a subject of debate [48,49]. In the oral context, SLe<sup>A/X</sup> have been the focus of study due to changes in their levels of expression during oral cancer [50,51], making this association with periodontal bacteria intriguing in the context of oral cancer exacerbation. Indeed, it would be interesting to repeat our experiments on primary normal cells, although it is likely that results would be similar given the finding by Honma et al., that sialic acid is important for invasion of and survival within normal oral keratinocytes [7,15].

In addition to cell surfaces, the sialylated and non-sialylated Lewis isomers are known to be present in secreted glycoproteins, including salivary mucins [52,53]. Considering the apparent abundance of SLe<sup>A/X</sup> in the oral cavity, it is logical that *T. forsythia* NanH would have evolved with the capability of targeting these and other ligands.

Taken overall, these data indicate that SLe antigens are important in host-pathogen interactions of *T. forsythia*, while these data open the possibility that glycan mimics could act as a method to prevent bacterial infections in the context of periodontal disease, but also for other pathogens that rely on sialylated surface antigens for cell-surface interactions during infection. One area where anti-infective and anti-inflammatory properties of sialylated oligosaccharide glycans has been postulated is their presence in human milk, as Human Milk Oligosaccharides (HMOs) where their beneficial influence on gut health via anti-inflammatory and anti-infective properties against gastro-intestinal pathogens has been revealed [54–56].

## CONCLUSION

In this paper, we set out to further investigate the role of sialidase in the pathogenicity of *T.*

forsythia, examining and confirming the role of a novel CBM whose avidity for a broad range of oligosaccharides is enhanced by its partner catalytic domain. We believe that this domain, represents a potentially new subfamily of CBM's, distinct from that of the *V. cholerae* sialidase CBM40 domain, the founding member of the only other sialic acid related CBM subfamily [25]. We also establish the role of Lewis antigens (SLe<sup>A</sup> and SLe<sup>X</sup>) both as catalytic substrates and ligands for the NanH-CBM, and also as key ligands for host-pathogen interactions during cellular invasion. This raises the possibility that free oligosaccharides or synthetic analogues could prove useful as antimicrobial agents that prevent invasion of bacteria into cells. These may be useful in conjunction with current sialidase inhibitors (e.g. Tamiflu / oseltamivir, and Relenza / zanamivir) that function by competitive inhibition of the active site. One other approach may be inhibitors that bind bacterial CBMs directly, a possibility we are currently investigating in studies using compound libraries and structure-based approaches.

In addition, given the apparent importance of sialidases in the biology of periodontal and other pathogenic organisms, e.g. *V. cholerae* and *S. pneumoniae* [57–59] we suggest that an approach targeting sialometabolism (via sialidases) may have broad applicability for a range of infections at mucosal interfaces. It is also true that periodontal disease is polymicrobial in nature, characterised by a dysbiosis where certain pathogens occur in higher numbers and possess community attributes that cause disease. Among these attributes one can almost certainly consider sialidase activity, given increased sialidase activity in periodontal communities and nanH gene transcription in vivo [16,60]. This raises the novel possibility that targeting sialidase activity as well as its ligand-binding ability, might be an aspect of the bacterial community worth manipulating to move away from or prevent dysbiosis, improving disease outcomes or preventing the onset of this common condition.

## ACKNOWLEDGEMENTS

We wish to thank Floyd Dewhirst for the 92A.2 strain. Work was funded by a BBSRC iCASE awards (with GlaxoSmithKline (BB/K501098/1), and BB/M01570X/1) to Graham Stafford, and Dunhill Medical Trust grant DMT-R185/0211 to Graham Stafford. We also acknowledge Ashu Sharma(SUNY,USA) for critical reading.

## REFERENCES

- 1 Socransky, S. S., Haffajee, A. D., Cugini, M. A., Smith, C. and Kent RL Jr. (1998) Microbial complexrs in subgingival plaque. *J Clin Periodontol* **25**, 134–144.
- 2 Sharma, A. (2011) Virulence mechanisms of *Tannerella forsythia*. *Periodontol.* 2000 **54**, 106–116.

- 3 Wyss, C. (1989) Dependence of proliferation of *Bacteroides forsythus* on exogenous N-acetylmuramic acid. *Infect. Immun.* **57**, 1757–1759.
- 4 Roy, S., Douglas, C. W. I. and Stafford, G. P. (2010) A novel sialic acid utilization and uptake system in the periodontal pathogen *Tannerella forsythia*. *J. Bacteriol.* **192**, 2285–2293.
- 5 Stafford, G., Roy, S., Honma, K. and Sharma, A. (2012) Sialic acid, periodontal pathogens and *Tannerella forsythia*: Stick around and enjoy the feast! *Mol. Oral Microbiol.* **27**, 11–22.
- 6 Phansopa, C., Roy, S., Rafferty, J. B., Douglas, C. W. I., Pandhal, J., Wright, P. C., Kelly, D. J. and Stafford, G. P. (2014) Structural and functional characterization of NanU, a novel high-affinity sialic acid-inducible binding protein of oral and gut-dwelling *Bacteroidetes* species. *Biochem. J.* **458**, 499–511.
- 7 Honma, K., Ruscitto, A., Frey, A. M., Stafford, G. P. and Sharma, A. (2015) Sialic acid transporter NanT participates in *Tannerella forsythia* biofilm formation and survival on epithelial cells. *Microb. Pathog., Elsevier Ltd* **94**, 12–20.
- 8 Lewis, A. L. and Lewis, W. G. (2012) Host sialoglycans and bacterial sialidases: A mucosal perspective. *Cell. Microbiol.* **14**, 1174–1182.
- 9 Douglas, C. W. I., Naylor, K., Phansopa, C., Frey, A. M., Farmilo, T. and Stafford, G. P. (2014) Physiological adaptations of key oral bacteria. *Adv. Microb. Physiol.* (Poole, R. K., ed.), AMP, UK, Academic Press **65**, 257–335.
- 10 Corfield, T. (1992) Bacterial sialidases--roles in pathogenicity and nutrition. *Glycobiology* **2**, 509–21.
- 11 Monti, E. and Miyagi, T. (2015) Structure and Function of Mammalian Sialidases. In *SialoGlyco Chemistry and Biology I: Biosynthesis, structural diversity and sialoglycopathologies*, pp 183–208.
- 12 Muñoz-Barroso, I., García-Sastre, a, Villar, E., Manuguerra, J. C., Hannoun, C. and Cabezas, J. a. (1992) Increased influenza A virus sialidase activity with N-acetyl-9-O-acetylneuraminic acid-containing substrates resulting from influenza C virus O-acetylerase action. *Virus Res.* **25**, 145–53.
- 13 Li, C., Kurniyati, Hu, B., Bian, J., Sun, J., Zhang, W., Liu, J., Pan, Y. and Li, C. (2012) Abrogation of neuraminidase reduces biofilm formation, capsule biosynthesis, and virulence of *Porphyromonas gingivalis*. *Infect. Immun.* **80**, 3–13.
- 14 Kurniyati, K., Zhang, W., Zhang, K. and Li, C. (2013) A surface-exposed neuraminidase affects complement resistance and virulence of the oral spirochaete *Treponema denticola*. *Mol. Microbiol.* **89**, 842–856.
- 15 Honma, K., Mishima, E. and Sharma, A. (2011) Role of *tannerella forsythia* nanH sialidase in epithelial cell attachment. *Infect. Immun.* **79**, 393–401.
- 16 Gul, S. S., Griffiths, G. S., Stafford, G. P., Al-Zubidi, M. I., Rawlinson, A. and Douglas, C. W. I. (2017) Investigation of a Novel Predictive Biomarker Profile for the Outcome of Periodontal Treatment. *J. Periodontol.*
- 17 Roy, S., Honma, K., Douglas, I., Sharma, A., Stafford, G. P., Douglas, C. W. I., Sharma, A. and Stafford, G. P. (2011) Role of sialidase in glycoprotein utilisation by *Tannerella forsythia*. *Microbiology* **157**, 3195–3202.
- 18 Thompson, H., Homer, K. A., Rao, S., Booth, V. and Hosie, A. H. F. (2009) An orthologue of *Bacteroides fragilis* NanH is the principal sialidase in *Tannerella forsythia*. *J. Bacteriol.* **191**, 3623–3628.
- 19 Stafford, P., Higham, J., Pinnock, A., Murdoch, C., Douglas, C. W. I., Stafford, G. P. and Lambert, D. W. (2013) Gingipain-dependent degradation of mammalian target of rapamycin pathway proteins by the periodontal pathogen *Porphyromonas gingivalis* during invasion. *Mol. Oral Microbiol.* **28**, 366–378.
- 20 Aminoff, D. (1961) Methods for the quantitative estimation of N-acetylneuraminic acid and their application to hydrolysates of sialomucoids. *Biochem. J.* **81**, 384–92.
- 21 Romero, E. L., Pardo, M. F., Porro, S. and Alonso, S. (1997) Sialic acid measurement by a modified Aminoff method: a time-saving reduction in 2-thiobarbituric acid concentration. *J.*

- Biochem. Biophys. Methods **35**, 129–34.
- 22 Schindelin, J., Arganda-Carreras, I., Frise, E., Kaynig, V., Longair, M., Pietzsch, T., Preibisch, S., Rueden, C., Saalfeld, S., Schmid, B., et al. (2012) Fiji: An open-source platform for biological-image analysis. *Nat. Methods* **9**, 676–682.
- 23 Crennell, S., Garman, E., Laver, G., Vimr, E. and Taylor, G. (1994) Crystal structure of *Vibrio cholerae* neuraminidase reveals dual lectin-like domains in addition to the catalytic domain. *Structure* **2**, 535–44.
- 24 Roggentin, P., Schauer, R., Hoyer, L. L. and Vimr, E. R. (1993) The sialidase superfamily and its spread by horizontal gene transfer. *Mol. Microbiol.* **9**, 915–21.
- 25 Lombard, V., Golaconda Ramulu, H., Drula, E., Coutinho, P. M. and Henrissat, B. (2014) The carbohydrate-active enzymes database (CAZy) in 2013. *Nucleic Acids Res.* **42**, D490–5.
- 26 Buschiazzo, A. and Alzari, P. M. (2008) Structural insights into sialic acid enzymology. *Curr. Opin. Chem. Biol.* **12**, 565–72.
- 27 Bickel, M. and Cimasoni, G. (1985) The pH of human crevicular fluid measured by a new microanalytical technique. *J. Periodontal Res.* **20**, 35–40.
- 28 Eggert, F. M., Drewell, L., Bigelow, J. A., Speck, J. E. and Goldner, M. (1991) The pH of gingival crevices and periodontal pockets in children, teenagers and adults. *Arch. Oral Biol.* **36**, 233–238.
- 29 Galgut, P. (2001) The relevance of pH to gingivitis and periodontitis. *J. Int. Acad. Periodontol.* 61–67.
- 30 Edgar, W. M. (1982) Duration of Response and Stimulus Sequence in the Interpretation of Plaque pH Data. *J. Dent. Res.* **61**, 1126–1129.
- 31 Takahashi, N. and Yamada, T. (1999) Effects of pH on the glucose and lactate metabolisms by the washed cells of *Actinomyces naeslundii* under anaerobic and aerobic conditions. *Oral Microbiol. Immunol.* **14**, 60–65.
- 32 Vroom, J. M., Grauw, K. J. De, Gerritsen, H. C., Bradshaw, D. J., Marsh, P. D., Watson, G. K., Birmingham, J., Allison, C. and Grauw, K. J. D. E. (1999) Depth Penetration and Detection of pH Gradients in Biofilms by Two-Photon Excitation Microscopy. *Appl. Environ. Microbiol.* **65**, 3502–3511.
- 33 Edlund, A., Yang, Y., Hall, A. P., Guo, L., Lux, R., He, X., Nelson, K. E., Neelson, K. H., Yooseph, S., Shi, W., et al. (2013) An in vitro biofilm model system maintaining a highly reproducible species and metabolic diversity approaching that of the human oral microbiome. *Microbiome* **1**, 1.
- 34 Zilm, P. S., Mira, A., Bagley, C. J. and Rogers, A. H. (2010) Effect of alkaline growth pH on the expression of cell envelope proteins in *Fusobacterium nucleatum*. *Microbiology* **156**, 1783–94.
- 35 Takahashi, N. (2003) Acid-neutralizing activity during amino acid fermentation by *Porphyromonas gingivalis*, *Prevotella intermedia* and *Fusobacterium nucleatum*. *Oral Microbiol. Immunol.* **18**, 109–13.
- 36 Potempa, J., Mikolajczyk-Pawlinska, J., Brassell, D., Nelson, D., Thøgersen, I. B., Enghild, J. J. and Travis, J. (1998) Comparative properties of two cysteine proteinases (gingipains R), the products of two related but individual genes of *Porphyromonas gingivalis*. *J. Biol. Chem.* **273**, 21648–57.
- 37 Karim, A., Kulczycka, M., Kantyka, T., Dubin, G., Jabaiah, A., Daugherty, P., Thøgersen, I., Enghild, J. J., Nguyen, K.-A. and Potempa, J. (2010) A Novel Matrix Metalloprotease-like Enzyme (Karilysin) of the Periodontal Pathogen *Tannerella forsythia* ATCC 43037. *Biol. Chem.* **391**, 1442–1448.
- 38 Phansopa, C., Kozak, R. P., Liew, L. P., Frey, A. M., Farmilo, T., Parker, J. L., Kelly, D. J., Emery, R. J., Thomson, R. I., Royle, L., et al. (2015) Characterization of a sialate-O-acetyltransferase (NanS) from the oral pathogen *Tannerella forsythia* that enhances sialic acid release by NanH, its cognate sialidase. *Biochem. J.* **472**, 157–167.

- 39 Bergstrom, K. S. B. and Xia, L. (2013) Mucin-type O-glycans and their roles in intestinal homeostasis. *Glycobiology* **23**, 1026–1037.
- 40 Croce, M. V., Isla-Larrain, M., Rabassa, M. E., Demichelis, S., Colussi, A. G., Crespo, M., Lacunza, E. and Segal-Eiras, A. (2007) Lewis x is Highly Expressed in Normal Tissues: a Comparative Immunohistochemical Study and Literature Revision. *Pathol.Oncol.Res.*, Centre of Basic and Applied Immunological Research (CINIBA), Faculty of Medical Sciences, UNLP, La Plata, Argentina **13**, 130–138.
- 41 Moustafa, I., Connaris, H., Taylor, M., Zaitsev, V., Wilson, J. C., Kiefel, M. J., Von Itzstein, M. and Taylor, G. (2004) Sialic acid recognition by *Vibrio cholerae* neuraminidase. *J. Biol. Chem.* **279**, 40819–40826.
- 42 Xu, G., Potter, J. A., Russell, R. J. M., Oggioni, M. R., Andrew, P. W. and Taylor, G. L. (2008) Crystal Structure of the NanB Sialidase from *Streptococcus pneumoniae*. *J. Mol. Biol.* **384**, 436–449.
- 43 Owen, C. D., Lukacik, P., Potter, J. A., Sleator, O., Taylor, G. L. and Walsh, M. A. (2015) *Streptococcus pneumoniae* NanC: Structural insights into the specificity and mechanism of a sialidase that produces a sialidase inhibitor. *J. Biol. Chem.* **290**, 27736–27748.
- 44 Ribeiro, J. P., Pau, W. K., Pifferi, C., Renaudet, O., Varrot, A., Mahal, L. K. and Imberty, A. (2016) Characterization of a high-affinity sialic acid specific CBM40 from *Clostridium perfringens* and engineering of divalent form. *Biochem. J.* **473**, 2109–2118.
- 45 Chien, C.-H., Shann, Y.-J. and Sheu, S.-Y. (1996) Site-directed mutation of the catalytic and conserved amino acids of the neuraminidase gene, nanH, of *Clostridium perfringens* ATCC 10543. *Enzyme Microb. Technol.* **19**, 267–276.
- 46 Suwannakul, S., Stafford, G. P., Whawell, S. A. and Douglas, C. W. I. (2010) Identification of bistable populations of *Porphyromonas gingivalis* that differ in epithelial cell invasion. *Microbiology* **156**, 3052–3064.
- 47 Lowe, J. B. (2003) Glycan-dependent leukocyte adhesion and recruitment in inflammation. *Curr. Opin. Cell Biol.* **15**, 531–538.
- 48 Moughal, N. A., Adonogianaki, E., Thornhill, M. H. and Kinane, D. F. (1992) Endothelial cell leukocyte adhesion molecule-1 (ELAM-1) and intercellular adhesion molecule-1 (ICAM-1) expression in gingival tissue during health and experimentally-induced gingivitis. *J. Periodontal Res.* **27**, 623–30.
- 49 Pietrzak, E. R., Savage, N. W., Aldred, M. J. and Walsh, L. J. (1996) Expression of the E-selectin gene in human gingival epithelial tissue. *J. oral Pathol. Med.* **25**, 320–324.
- 50 Renkonen, J., Makitie, A., Paavonen, T. and Renkonen, R. (1999) Sialyl-Lewis x/a - decorated selectin ligands in head and neck tumours. *J. Cancer Res. Clin. Oncol.* **125**, 569–576.
- 51 Wiest, I., Alexiou, C., Mayr, D., Schulze, S., Kuhn, C., Kunze, S., Buttner, M., Betz, P. and Jeschke, U. (2010) Expression of the carbohydrate tumor marker Sialyl Lewis a (Ca19-9) in squamous cell carcinoma of the larynx. *Anticancer Res.* **30**, 1849–1853.
- 52 Zalewska, A., Zwierz, K., Zólkowski, K. and Gindzieński, A. (2000) Structure and biosynthesis of human salivary mucins. *Acta Biochim. Pol.* **47**, 1067–1079.
- 53 Prakobphol, A., Thomsson, K. A., Hansson, G. C., Rosen, S. D., Singer, M. S., Phillips, N. J., Medzihradzky, K. F., Burlingame, A. L., Leffler, H. and Fisher, S. J. (1998) Human Low-Molecular-Weight Salivary Mucin Expresses the Sialyl Lewis x Determinant and Has L-Selectin Ligand Activity. *Biochemistry* **37**, 4916–4927.
- 54 Ten Bruggencate, S. J., Bovee-Oudenhoven, I. M., Feitsma, A. L., van Hoffen, E. and Schoterman, M. H. (2014) Functional role and mechanisms of sialyllactose and other sialylated milk oligosaccharides. *Nutr. Rev.* **72**, 377–389.
- 55 Bode, L. and Jantscher-krenn, E. (2012) Structure-Function Relationships of Human Milk Oligosaccharides. *Adv. Nutr.* **3**, 383–391.
- 56 Kunz, C. and Rudloff, S. (2008) Potential Anti-inflammatory and Anti-Infectious Effects of Human Milk Oligosaccharides. *Adv. Exp. Med. Biol.* **606**, 455–465.

- 57 Galen, J. E., Ketley, J. M., Fasano, A., Richardson, S. H., Wasserman, S. S. and Kaperl, J. B. (1992) Role of *Vibrio cholerae* Neuraminidase in the Function of Cholera Toxin. *Infect. Immun.* **60**, 406–415.
- 58 Almagro-Moreno, S. and Boyd, E. F. (2009) Sialic acid catabolism confers a competitive advantage to pathogenic *Vibrio cholerae* in the mouse intestine. *Infect. Immun.* **77**, 3807–3816.
- 59 Manco, S., Hernon, F., Yesilkaya, H., Paton, J. C., Andrew, P. W. and Kadioglu, A. (2006) Pneumococcal neuraminidases A and B both have essential roles during infection of the respiratory tract and sepsis. *Infect. Immun.* **74**, 4014–4020.
- 60 Duran-Pinedo, A. E., Chen, T., Teles, R., Starr, J. R., Wang, X., Krishnan, K. and Frias-Lopez, J. (2014) Community-wide transcriptome of the oral microbiome in subjects with and without periodontitis. *ISME J.* **8**, 1659–72.
- 61 Gut, H., King, S. J. and Walsh, M. A. (2008) Structural and functional studies of *Streptococcus pneumoniae* neuraminidase B: An intramolecular trans-sialidase. *FEBS Lett., Federation of European Biochemical Societies* **582**, 3348–3352.
- 62 Xu, G., Kiefel, M. J., Wilson, J. C., Andrew, P. W., Oggioni, M. R. and Taylor, G. L. (2011) Three streptococcus pneumoniae sialidases: Three different products. *J. Am. Chem. Soc.* **133**, 1718–1721.
- 63 Cacalano, G., Kays, M., Saiman, L. and Prince, A. (1992) Production of the *Pseudomonas aeruginosa* neuraminidase is increased under hyperosmolar conditions and is regulated by genes involved in alginate expression. *J. Clin. Invest.* **89**, 1866–1874.
- 64 Mizan, S., Henk, A., Stallings, A., Maier, M. and Lee, M. D. (2000) Cloning and characterization of sialidases with 2-6' and 2-3' sialyl lactose specificity from *Pasteurella multocida*. *J. Bacteriol.* **182**, 6874–6883.
- 65 Kim, S., Oh, D. B., Kwon, O. and Kang, H. A. (2010) Identification and functional characterization of the NanH extracellular sialidase from *Corynebacterium diphtheriae*. *J. Biochem.* **147**, 523–533.
- 66 Li, J. and McClane, B. a. (2013) The Sialidases of *Clostridium perfringens* Type D Strain CN3718 Vary in Their Properties and Sensitivity to Inhibitors. *Appl. Environ. Microbiol.* **80**, 1701–1709.
- 67 Hoyer, L. L., Roggentin, P., Schauer, R. and Vimr, E. R. (1991) Purification and properties of cloned *Salmonella typhimurium* LT2 sialidase with virus-typical kinetic preference for sialyl alpha 2-3 linkages. *J. Biochem.* **110**, 462–7.
- 68 Park, K.-H., Kim, M.-G., Ahn, H.-J., Lee, D.-H., Kim, J.-H., Kim, Y.-W. and Woo, E.-J. (2013) Structural and biochemical characterization of the broad substrate specificity of *Bacteroides thetaiotaomicron* commensal sialidase. *Biochim. Biophys. Acta, Elsevier B.V.* **1834**, 1510–9.
- 69 Tailford, L. E., Owen, C. D., Walshaw, J., Crost, E. H., Hardy-Goddard, J., Le Gall, G., De Vos, W. M., Taylor, G. L. and Juge, N. (2015) Discovery of intramolecular trans-sialidases in human gut microbiota suggests novel mechanisms of mucosal adaptation. *Nat. Commun., Nature Publishing Group* **6**, 1–12.
- 70 Byers, H. L., Tarelli, E., Homer, K. A. and Beighton, D. (2000) Isolation and characterisation of sialidase from a strain of *Streptococcus oralis*. *J. Med. Microbiol.* **49**, 235–244.
- 71 Johnston, C., Hinds, J., Smith, A., Van Der Linden, M., Van Eldere, J. and Mitchell, T. J. (2010) Detection of large numbers of pneumococcal virulence genes in streptococci of the mitis group. *J. Clin. Microbiol.* **48**, 2762–2769.
- 72 Ceroni, A., Maass, K., Geyer, H., Geyer, R., Dell, A. and Haslam, S. M. (2008) GlycoWorkbench: A tool for the computer-assisted annotation of mass spectra of glycans. *J. Proteome Res.* **7**, 1650–1659.

## FIGURE LEGENDS

**Figure 1. pH optima of NanH and whole *T. forsythia*.** MUNANA was incubated with NanH for 1 min or one of two *T. forsythia* strains for 30 min, in a variety of buffers with variable pH. Reactions were halted and the pH equalised by addition of an excess of sodium carbonate-bicarbonate buffer, pH 10.5. Sialidase activity catalysed the production of 4-MU from MU-NANA, which was quantified by measuring fluorescence of the reactions at excitation and emission wavelengths of 350 and 450 nm. (A) NanH, (B) *T. forsythia* NCTC 43037, (C) *T. forsythia* 92A2. Data shown represent the mean of two experiments where each condition was repeated three times per experiment. Error bars = S.D.

**Figure 2. Reaction kinetics of MU-NANA and NanH under different conditions.** Variable concentrations of MU-NANA were exposed to NanH, under different pH and salinity conditions. Reactions were quenched by addition of pH 10.5 buffer at 1, 2, and 3 min, and the rate of 4-MU release determined by application of a 4-MU standard curve. (A) Michaelis–Menten plot, rate of 4-MU release ( $V_0$ ,  $\mu\text{mol MU released}/\text{min}/\text{mg NanH}$ ), plotted against [MU-NANA] ( $\mu\text{M}$ ) using Prism 7 (GraphPad). Data shown represent mean of three experimental repeats for each condition, error bars = S.E.M. (B) Table summarising Michaelis-Menten reaction kinetics and catalytic efficiency of NanH and MU-NANA, the table includes the  $k_{\text{cat}}$  (4-MU release/min), and  $k_{\text{cat}}/K_M$  ( $\mu\text{M}/\text{min}$ ).

**Figure 3. Reaction kinetics of NanH with  $\alpha$ 2-3- and  $\alpha$ 2-6-linked sialic acid (sialyllactose) and SLe<sup>A</sup> and SLe<sup>X</sup> under physiological conditions.** Variable concentrations of 3- and 6-SL, and SLe<sup>A</sup> and SLe<sup>X</sup> were digested with NanH, reactions were stopped at different time points and immediately subjected to the TBA assay. Application of a standard curve enabled determination of the rate of Neu5Ac release. The reaction was performed in buffer intended to mimic physiological conditions; 50mM Sodium Phosphate, 200mM NaCl, pH 7.4. (A) Michaelis–Menten kinetics of NanH for 3- and 6-SL, and (B) SLe<sup>A</sup> and SLe<sup>X</sup>. For each substrate, representative data are shown with condition repeated three times per experiment. Error bars = S.E.M. (C) Table summarising Michaelis-Menten reaction kinetics and catalytic efficiency of NanH and 3-SL, 6-SL, SLe<sup>A</sup> or SLe<sup>X</sup>, the table includes the  $K_{\text{cat}}$  (4-MU release/min), and  $K_{\text{cat}}/K_M$  ( $\mu\text{M}/\text{min}$ ).

**Figure 4. Alignment of NanH-CBM.** Alignment and image production was performed using MultAlin and ESPript, and to establish similarity between aligned residues, percentage equivalence with a global score of 0.7 was used. Aligned sequences above the percentage equivalent threshold

are framed in blue, and aligned residues above this threshold are shown in red. Strictly conserved residues are shown in white on a red background. Alignment of the sialidase-CBMs from three *T. forsythia* (TF) strains (92.A2, ATCC 43037, and UB4), *Alistipes* sp., NCBI Taxonomy ID: 1262695, *Parabacteroides distasonis*, *Bacteroides thetaiotaomicron* (*B. theta*), and the two *B. fragilis* (*B. frag*) NanH sialidases from strain 9343. NCBI accession numbers were WP\_046826229.1, WP\_014225510.1, SCQ21971.1, CDD16645.1, WP\_036613805.1, WP\_055222135.1, CAH07505.1, CAH09725.1 respectively.

**Figure 5. Affinity of NanH-CBM for sialyl- and non-sialylated glycoconjugates.** NanH-CBM were exposed to substrates at different concentrations, after which the quenching of intrinsic tryptophan fluorescence was measured using a fluorescence spectrometer, at excitation 295 nm, emissions from 300–380 nm, with changes to fluorescence expressed relative to the no substrate condition. (A) Binding of 3- and 6-SL, and non-sialylated lactose, to NanH-CBM. (B) Binding of non-sialylated Le<sup>A</sup> and Le<sup>X</sup> to NanH-CBM, (C) Binding of SLe<sup>A</sup> and SLe<sup>X</sup> to NanH-CBM. (D) Summary of K<sub>d</sub> data for NanH-CBM and all ligands tested. Data shown represent the mean (± S.D.) of one experiment, where each condition was repeated three times.

**Figure 6. Affinity of NanH-YMAP for 3- and 6-sialyllactose.** NanH-YMAP was exposed to 3- or 6-SL at different concentrations, after which the quenching of intrinsic tryptophan fluorescence was measured using a fluorescence spectrometer, at excitation 295 nm, emissions from 300–380 nm, with changes to fluorescence expressed relative to the no substrate condition. Data represent the mean of one experiment, where each condition was repeated three times. Statistical difference between the two data sets was assessed using an extra sum of squares F-test in GraphPad Prism, and the two datasets were found to be statistically different (i.e. applying a single curve to the two datasets is not the preferred model,  $P = 0.002$ ).

**Figure 7. NanH desialylates SLe<sup>A</sup> and SLe<sup>X</sup> on oral epithelial cells.** H357 cells were stained with (A) anti-SLe<sup>A</sup> or (B) anti-SLe<sup>X</sup> Ig (raised in mouse), followed by secondary staining with anti-mouse Ig-Alexa Flour 488 conjugate. Prior to staining, cells were treated with 50 nM NanH in PBS, or untreated — incubated with PBS alone. All images were visualised using the same microscopy and image processing parameters (fluorescence intensity, exposure time, and background subtraction). Images were captured in three fields of view, and this was repeated in three separate experiments. Images shown are representative of each condition. Quantification of cellular SLe<sup>A</sup> and SLe<sup>X</sup> was performed using the measurement function of Fiji (Image J) software to obtain the mean pixel intensity of the green channel (SLe<sup>A</sup>/SLe<sup>X</sup> staining), and this was divided by the cell count (number of nuclei) to obtain the mean fluorescence intensity (MFI)/cell. Error bars = S.E.M., Significance determined by paired *t*-test (\*\* $P = <0.01$ , \*\*\* $P = <0.001$ ).

**Figure 8. Association of *T. forsythia* with oral epithelial cells is influenced by (sialyl) Lewis sugars.** Antibiotic protection assays were performed, with *T. forsythia* used to infect the cell line H357 at a multiplicity of infection (MOI) of 1:100 host:bacterial cells, in the presence or absence of 10 nM Le<sup>X</sup>, SLe<sup>X</sup>, Le<sup>A</sup>, or SLe<sup>A</sup>, as described in methods. The % of total association (A), Attachment (B) and cellular Invasion (C) are expressed as % of total viable input bacteria. Data shown represent the mean of two experimental biological repeats, where each condition was performed twice per experiment with three wells. Error bars = S.E.M. Statistically significant differences between all conditions were tested using repeated measures one way ANOVA with Bonferroni correction for multiple comparisons.

## Tables

Site of Infection	Organism	Sialidase	Linkages Targeted	Linkage Preference	Reference
Respiratory tract	<i>Streptococcus pneumoniae</i>	NanA	$\alpha$ 2-3, $\alpha$ 2-6	$\alpha$ 2-6	[61]
		NanB	$\alpha$ 2-3	$\alpha$ 2-3	[61]
		NanC	$\alpha$ 2-3	$\alpha$ 2-3	[62]
	<i>Pseudomonas aeruginosa</i>	PAO1 neuraminidase	$\alpha$ 2-3, $\alpha$ 2-6	unknown	[63]
	<i>Pasturella multocida</i>	NanB	( $\alpha$ 2-3), $\alpha$ 2-6	$\alpha$ 2-6	[64]
		NanH	$\alpha$ 2-3, ( $\alpha$ 2-6)	$\alpha$ 2-3	[64]
<i>Corynebacterium diphtheriae</i>	NanH	$\alpha$ 2-3, $\alpha$ 2-6	$\alpha$ 2-6	[65]	
Gastrointestinal tract	<i>Clostridium perfringens</i>	NanI	$\alpha$ 2-3, $\alpha$ 2-6	$\alpha$ 2-3	[66]
		NanJ	$\alpha$ 2-3, $\alpha$ 2-6	$\alpha$ 2-6	[66]
		NanH	$\alpha$ 2-3, $\alpha$ 2-6	$\alpha$ 2-3	[66]
	<i>Salmonella Typhimurium</i>	NanH	$\alpha$ 2-3, $\alpha$ 2-6	$\alpha$ 2-3	[67]
	<i>Bacteroides thetaiotaomicron</i>	VPI-5482	$\alpha$ 2-3, $\alpha$ 2-6	$\alpha$ 2-6	[68]
	<i>Ruminococcus gnavus</i>	NanH	$\alpha$ 2-3	$\alpha$ 2-3	[69]
Oral cavity	<i>Porphyromonas gingivalis</i>	SiaPG	$\alpha$ 2-3, $\alpha$ 2-6	unknown	[13]
	<i>Treponema denticola</i>	TDE0471	$\alpha$ 2-3, $\alpha$ 2-6	unknown	[14]
	<i>Tannerella forsythia</i>	NanH	$\alpha$ 2-3, $\alpha$ 2-6	$\alpha$ 2-3	This study, [18]
	<i>Streptococcus oralis</i>	NanA	$\alpha$ 2-3, $\alpha$ 2-6	$\alpha$ 2-3	[70]
	<i>Streptococcus mitis</i> <sup>^</sup>	NanA*	$\alpha$ 2-3, $\alpha$ 2-6*	unknown	[71]

**Table 1. Sialic acid-linkage preferences of sialidases from bacteria associated with different mucosal sites.** *P. multocida* is a respiratory pathogen of cattle, and can cause wound infections in humans. \*Not all *S. mitis* isolates possess sialidase activity, and the ability to target both sialic acid linkages is unknown, but presumably both  $\alpha$ 2-3 and  $\alpha$ 2-6 linkages can be targeted, as inferred by its homology with NanA from other Streptococci.

**Supplementary figure S1. Linear Schematic of *T. forsythia* NanH.** The N- and C-terminal ends are indicated. Features include the secretion signal (SS, pink), carbohydrate binding module (CBM, blue), the sialidase domain (green). Other features are also shown; FRIP = FRIP motif, D = Asp boxes.

**Supplementary figure S2. Alignment of NanH from *T. forsythia* strains ATCC 43037 and 92.A2.** Alignment and image production was performed using MultAlin and ESPript, and to establish similarity between aligned residues, percentage equivalence with a global score of 0.5 was used. Aligned sequences above the percentage equivalent threshold are framed in blue, and aligned residues above this threshold are shown in red. Strictly conserved residues are shown in white on a red background. The consensus sequence is shown below. The secretion signal sequence—CBM and CBM—active site domain boundaries are delineated by black lines at residues 19 and 183, respectively. The FRIP motif is highlighted in a green box, and Asp-boxes in purple. Sequences obtained from NCBI, accession numbers for ATCC 43037 and 92.A2 were WP\_046826229.1 and WP\_014225510.1, respectively

**Supplementary figure S3. Purified NanH.** SDS-PAGE (12% polyacrylamide gel) of NanH-CBM after affinity chromatography, pooling of NanH-CBM-containing fractions, and dialysis. MW standard, EZ run pre-stained protein Rec ladder (ThermoFisher Scientific).

**Supplementary figure S4. Graphic representation of 3- and 6-sialyllactose, sialyl Lewis A and sialyl Lewis X.** SLe<sup>A</sup> and SLe<sup>X</sup> are two isomers, comprised of the same backbone of galactose (Gal) and N-acetylglucosamine (GlcNAc), with  $\alpha$ 2-3 linked sialic acid (Neu5Ac) at Gal, and a fucose (Fuc) linked to GlcNAc. The differences between these two glycans are the Fuc linkage, which can be  $\alpha$ 3 or  $\alpha$ 4, and the GlcNAc-Gal linkage which can be  $\beta$ 1-4 or  $\beta$ 1-3, giving rise to sialyl Lewis A and sialyl Lewis X, respectively (SLe<sup>A</sup>; Neu5Ac, $\alpha$ 2-3Gal, $\beta$ 1-3(Fuc $\alpha$ 1-4)GlcNAc. SLe<sup>X</sup>; Neu5Ac, $\alpha$ 2-3Gal, $\beta$ 1-4(Fuc $\alpha$ 1-3)GlcNAc). Images rendered in GlycoWorkbench [72].

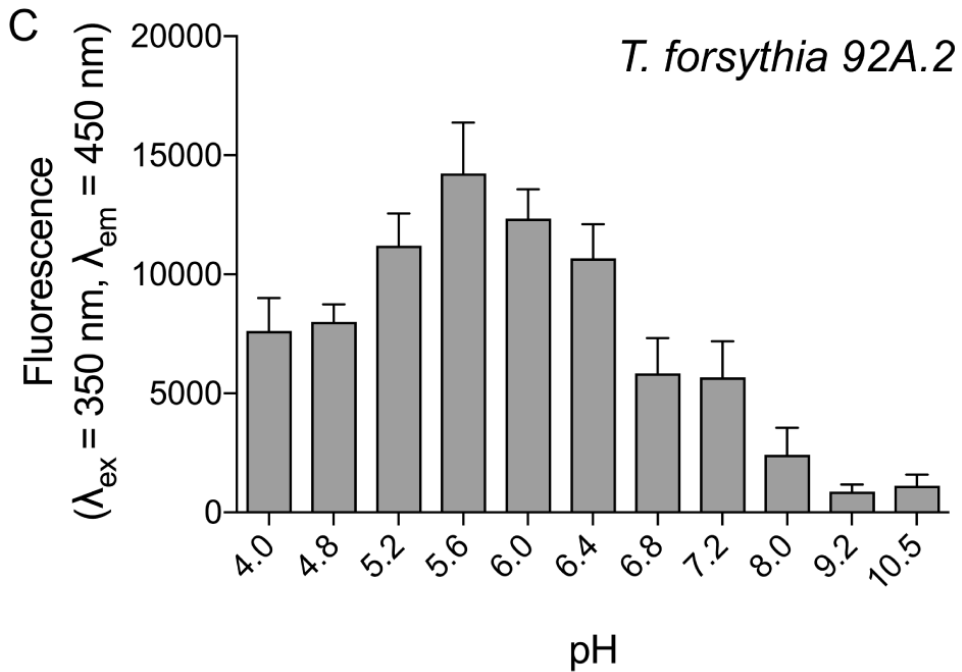
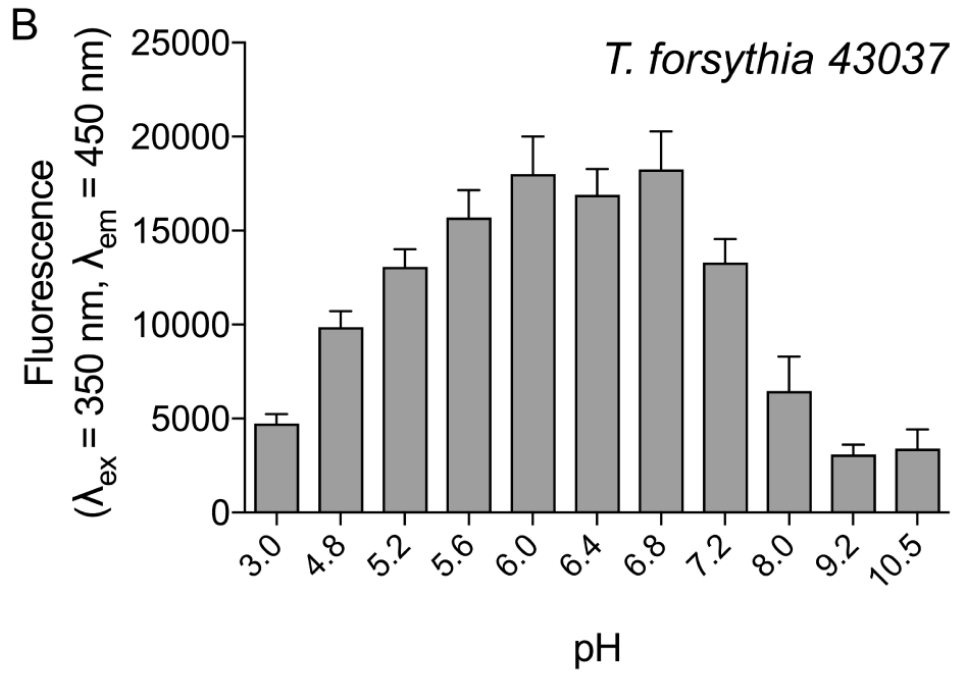
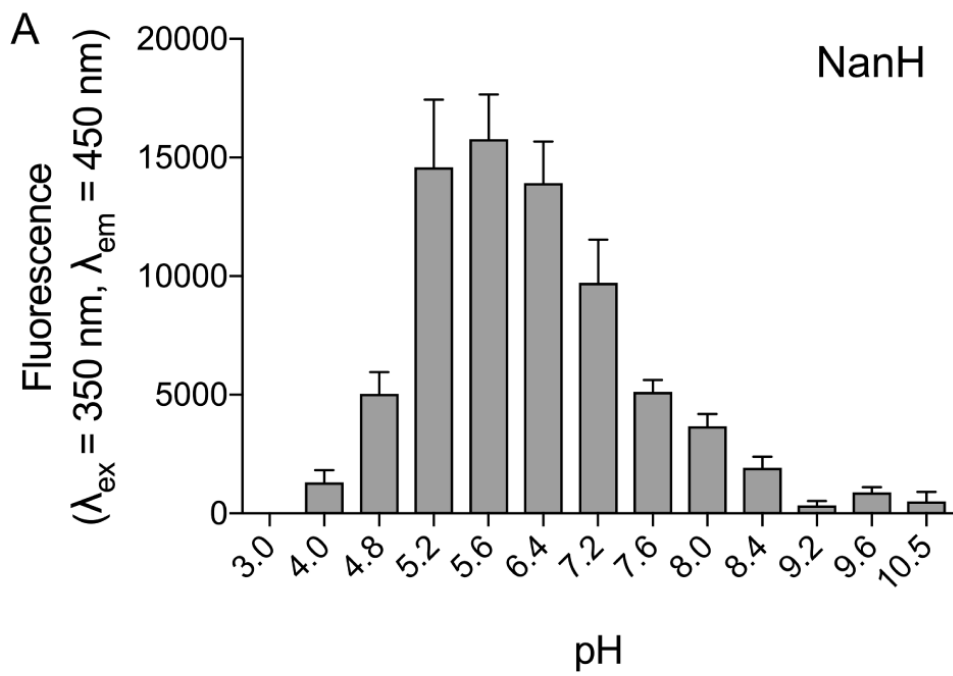
**Supplementary figure S5. Purified NanH-CBM.** SDS-PAGE (12% polyacrylamide gel) of NanH-CBM after affinity chromatography, pooling of NanH-CBM-containing fractions, and dialysis. MW standard, EZ run pre-stained protein Rec ladder (ThermoFisher Scientific).

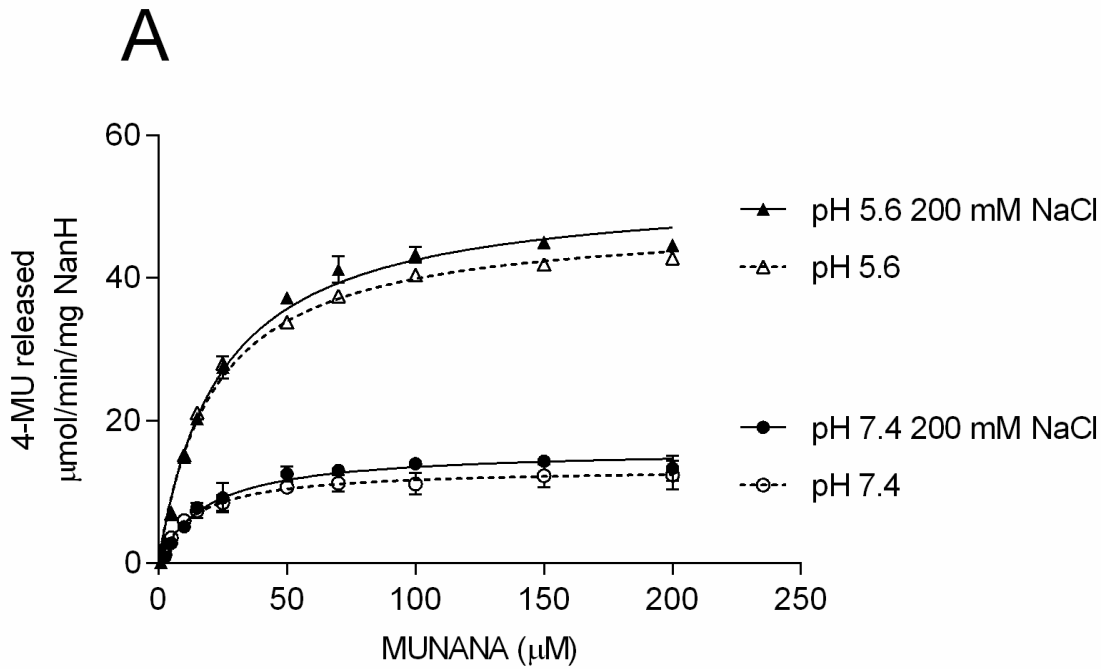
**Supplementary figure S6. Purification of NanH-YMAP, which lacks sialidase activity.** (A) SDS-PAGE (12% polyacrylamide gel) of NanH-YMAP after affinity chromatography, before

pooling of NanH-CBM-containing fractions. MW standard, EZ run pre-stained protein Rec ladder (ThermoFisher Scientific). (B) NanH or NanH-YMAP were exposed to MU-NANA for 1 and 10 min in the wells of a transparent 96-well plate before imaging under UV-light in a transilluminator. The apparent low-level fluorescence of NanH-YMAP in these images is likely due to UV-light fluorescence of protein. Negative control (–) was MU-NANA with no protein added.

**Supplementary figure S7. NanH desialylates oral epithelial cells.** H357 cells were stained with lectins for  $\alpha$ 2-6-linked and  $\alpha$ 2-3-linked sialic acid (SNA and MAA, visualised using FITC or Texas Red, respectively). Prior to staining, cells were treated with 50 nM NanH in PBS, or untreated (incubated with PBS only). All images were visualised using the same microscopy and image processing parameters (fluorescence intensity, exposure time, and background subtraction). Images were captured in three fields of view. Images shown are representative of each condition.

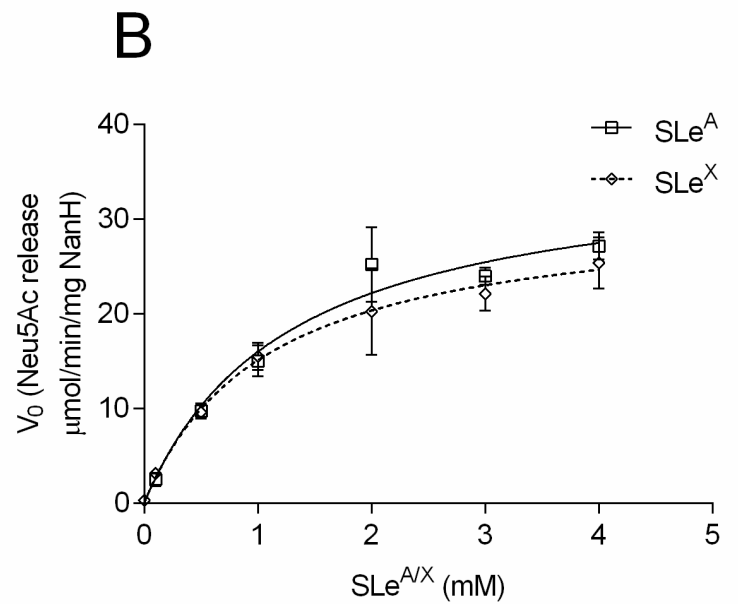
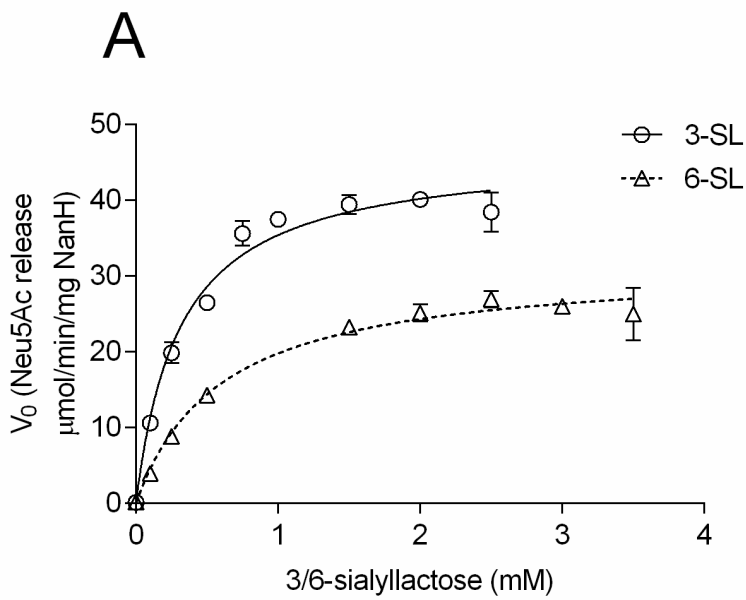
**Supplementary figure S8. NanH ligand binding-** NanH was exposed to 3- or 6-SL at different concentrations, after which the quenching of intrinsic tryptophan fluorescence was measured using a fluorescence spectrometer, at excitation 295 nm, emissions from 300–380 nm, with changes to fluorescence expressed relative to the no substrate condition. Data represent the mean of one representative experiment, where each condition was repeated three times.





**B**

	pH 7.4, 200 mM NaCl	pH 7.4	pH 5.6, 200 mM NaCl	pH 5.6
$k_{cat}$ (4-MU release/min)	922 ± 35.4	762.5 ± 29.9	3025 ± 54.03	2780 ± 45.76
$K_M$ ([MU-NANA], µM)	18.92 ± 2.65	13.81 ± 2.152	23.88 ± 1.45	21.37 ± 1.24
$k_{cat}/K_M$ (µM/min)	48.73	55.21	126.68	130.1
$V_{max}$ (4-MU release, µmol/min/mg NanH)	16.06 ± 0.61	13.28 ± 0.52	52.71 ± 0.94	48.42 ± 0.79



**C**

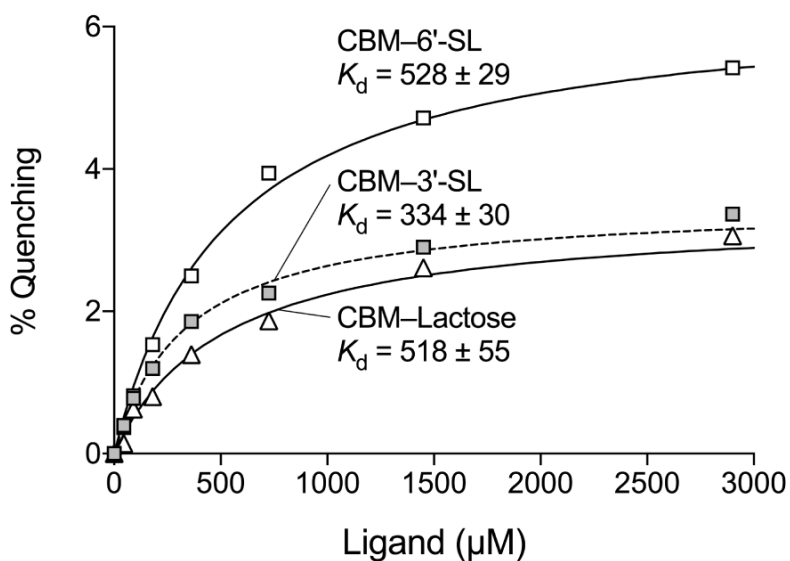
	3-SL	6-SL	$\text{SLe}^{\text{A}}$	$\text{SLe}^{\text{X}}$
$k_{\text{cat}}$ (4-MU release, min)	$2683 \pm 69.68$	$1823 \pm 55.64$	$2073 \pm 148.5$	$1793 \pm 122.1$
$K_M$ ([substrate], mM)	$0.31 \pm 0.03$	$0.60 \pm 0.07$	$1.26 \pm 0.24$	$1.07 \pm 0.21$
$k_{\text{cat}}/K_M$ (mM/min)	8655	3038	1645	1675
$V_{\text{max}}$ (Neu5Ac release, $\mu\text{mol}/\text{min}/\text{mg NanH}$ )	$46.44 \pm 1.21$	$31.56 \pm 0.96$	$36.11 \pm 2.59$	$31.24 \pm 2.13$

	1	10	20	30	40	50
TF_92A.2	.ADSVYV	QNPQIPILVDR	TDNVLF	RIRIPDAT	KGDVLNRLTIRF	GNEDKLSEVKAVRLFY
TF_43037	.ADSVYV	QNPQIPILIDRT	DNVLF	RIRIPDAT	KGDVLNRLTIRF	GNEDKLSEVKAVRLFY
TF_UB4	.ADSVYV	QNPQIPILIDRT	DNVLF	RIRIPDAT	KGDVLNRLTIRF	GNEDKLSEVKAVRLFY
Alistipes	ASDSLRIH	NPQIPILLDRM	DNVLF	QIRVPDAV	QGDVLES	LTVEFGPDTDIKSMAELRLFY
P.distastonis	.ADSLYVR	EQQIPILIDRI	DNVLYEM	RIP.AQ	KGDVLNEITIQI	GDNVNLSDIQAIRLFY
B.theta	ASDTVHVH	QTQIPILIER	QDNVLF	YFR	LDAKE	SRM.MDEIVLDFGKSVNLSDVQAVKLYY
B.frag_9343_nanH1	.ADTIFVR	ETRIPIER	QDNVLF	YLR	LDAKE	SQT.LNDVVLNLGEGVNLSEIQSIKLYY
B.frag_9343_nanH2	ATDTIFVY	ETQVPILIER	QDNMLF	LMRLTTA	RSDTKLNEVVLRL	GQNVNLSNIQSIKLYY
consensus>50	.aDsvy!	.#pq!PILi#R.	DNvL%	.iRipda.	kgdv\$#eitief	GnevnlsevqavrL%Y

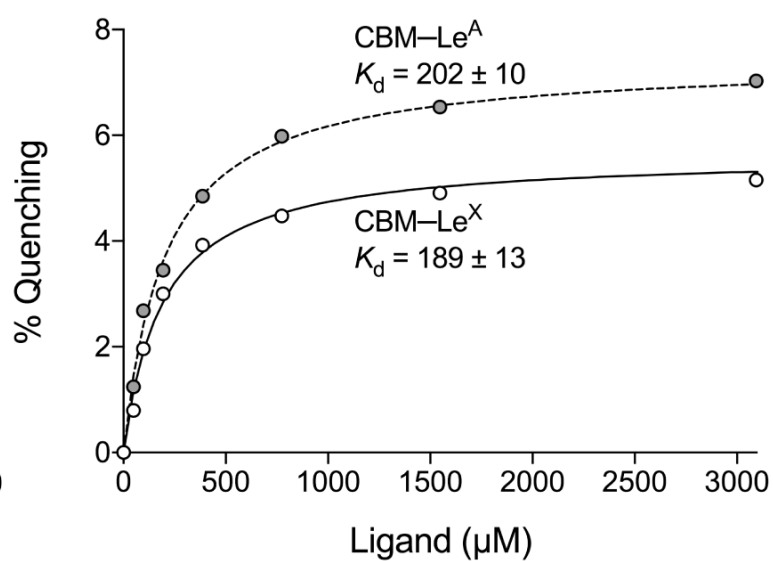
	60	70	80	90	100	110																		
TF_92A.2	A	GTEAATKGR.	S	RFAPVTYVSSHNI	RNT	TRSANPSYS	IRQDEVTT.	VAN	NTLT	LK	T	RQPMVK												
TF_43037	A	GTEAATKGR.	S	RFAPVTYVSSHNI	RNT	TRSANPSYS	VRQDEVTT.	AA	NTLT	LK	T	RQPMVK												
TF_UB4	A	GTEAATKGR.	S	RFAPVTYVSSHNI	RNT	TRSANPSYS	VRQDEVTT.	AA	NTLT	LK	T	RQPMVK												
Alistipes	S	GTEAVRRQG.	L	RFSPVEYIS	AHN	VWNT	TRSANPSYS	VMQE	QVSK.	I	GRKV	VV	LHS	RQPMVG										
P.distastonis	S	GVEAPSRKG.	E	HFS	PVTYIS	SHIP	GNT	TRKALE	SYS	VRQDEV	TTP	LS	RTV	KL	TSKQPMLK									
B.theta	G	GTEALQDKG	KK	RFAPVDYIS	SHRP	GNT	LA	AIP	SYS	IKCAE	V	LQP.	SA	KV	VV	LKS	HYK	LFP						
B.frag_9343_nanH1	G	GTEALQDSG	KK	RFAPVGYIS	SNT	PGK	T	LA	ANP	SYS	IKKSE	V	TNP.	G	NQ	VV	LK	G	DQ	K	LFP			
B.frag_9343_nanH2	G	GTEARQNYG	KE	LYLPVTYIS	RDV	SGK	T	LA	ANP	SYS	INKS	Q	V	NNP.	G	RK	V	I	L	N	A	NQ	K	LFP
consensus>50	.GtEA...	.g..r%aPvtY!	Sshnign	TrsAnpSYS!	rqd#Vttp.	.ntvvLk.	rqp\$vk																	

	120	130	140	150	160																																													
TF_92A.2	G	IN	YFWVS	VE	MDRNT	SL	LSKLT	S	TV	T	EVVIND	KPAVI.	AG	EQ	A.	AVRRMG	...																																	
TF_43037	G	IN	YFWVS	VE	MDRNT	SL	LSKLT	P	TV	T	EAVIND	KPAVI.	AG	EQ	A.	AVRRMG	I	GV	...																															
TF_UB4	G	IN	YFWVS	VE	MDRNT	SL	LSKLT	P	TV	T	EAVIND	KPAVI.	AG	EQ	A.	AVRRMG	I	GV	...																															
Alistipes	G	IN	YWVS	V	RMNP	DASL	LTEL	R	A	R	V	S	EV	V	N	G	K	K	I	P	V.	A	C	D	S	R	D	V	V	R	R	M	G	Y	G	V	R	H	A											
P.distastonis	G	IN	YFWVS	I	Q	M	K	P	E	T	S	L	L	A	K	V	A	T	T	I	P	N	A	Q	I	N	N	K	P	I	D	I.	T	W	K	G	K	V	D	E	R	H	V	G	...					
B.theta	G	IN	FFWIS	L	Q	M	K	P	E	T	S	L	F	T	K	I	S	S	E	L	Q	S	V	K	I	D	G	K	E	A	I	C	E	E	R	S	P	K	D	I	I	H	R	...						
B.frag_9343_nanH1	G	IN	YFWIS	L	Q	M	K	P	G	T	S	L	T	S	K	V	T	A	D	I	A	S	I	T	L	D	G	K	K	A	L	L	D	V	V	S	E	N	G	I	E	H	R	M	G	V	G	V	...	
B.frag_9343_nanH2	G	IN	YFWIS	L	Q	M	K	P	G	A	S	L	L	D	K	V	S	A	K	I	V	T	V	K	V	D	N	K	E	A	L	I	Y	T	V	S	P	E	N	I	T	H	R	V	G	V	G	V	R	...
consensus>50	GIN%%W!	SvqMdpnt	SLlskvt.	tv.	evvi#dKpavi.	a.eq.	.ivr	rmgigv...																																										

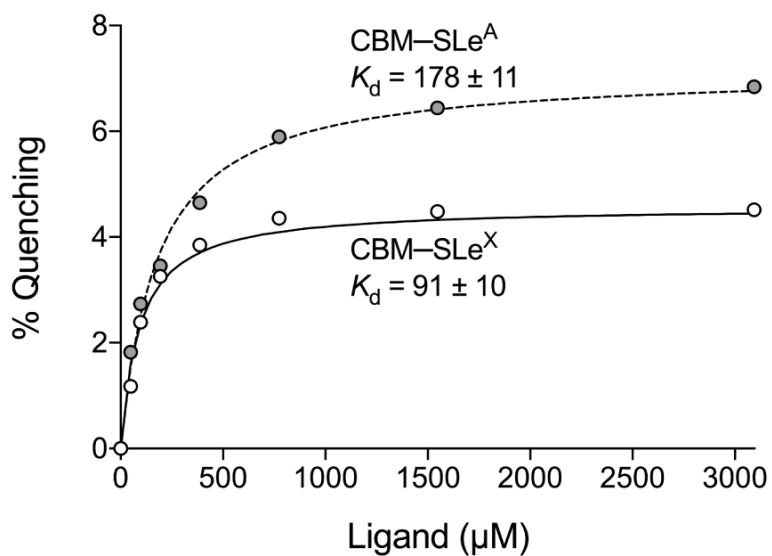
**A 3', 6'-Sialyllactose / Lactose**



**B Lewis<sup>X/A</sup>**



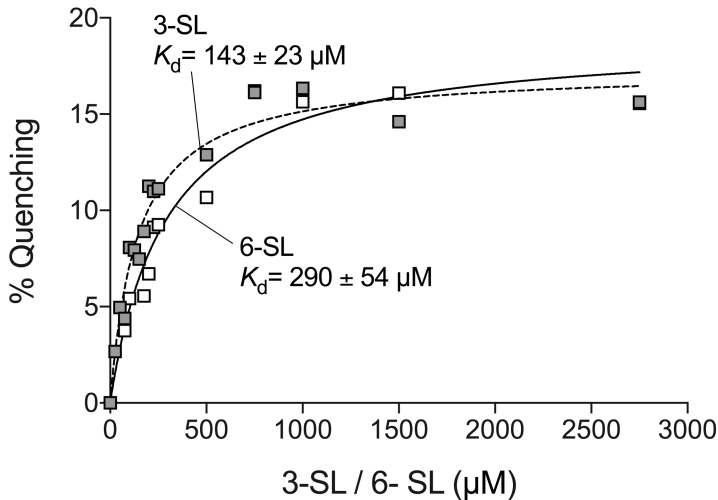
**C Sialyl Lewis<sup>X/A</sup>**

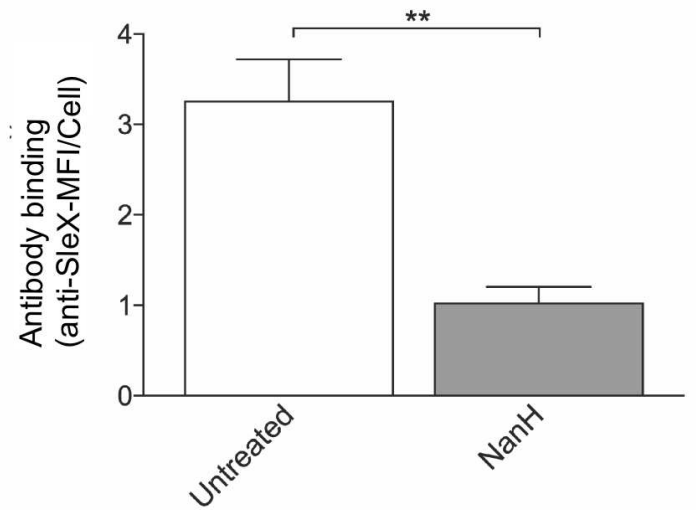
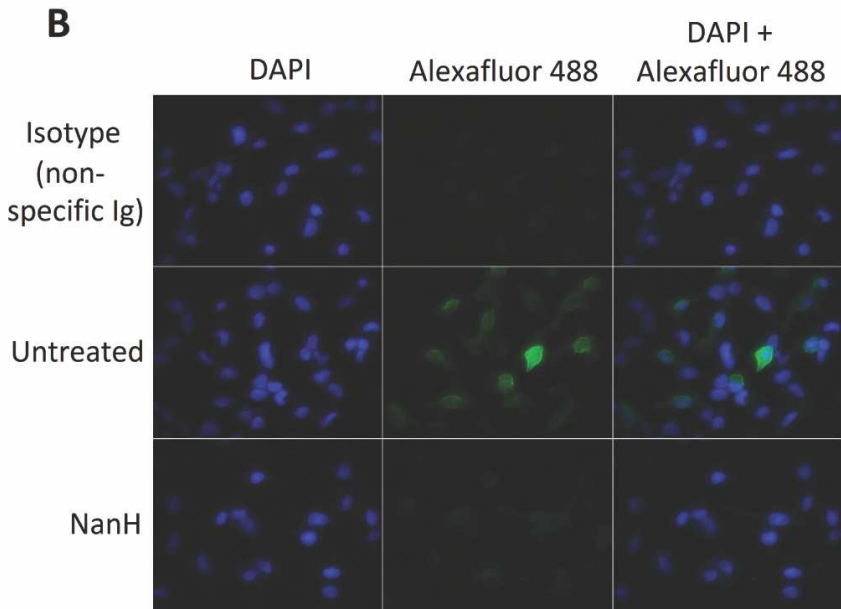
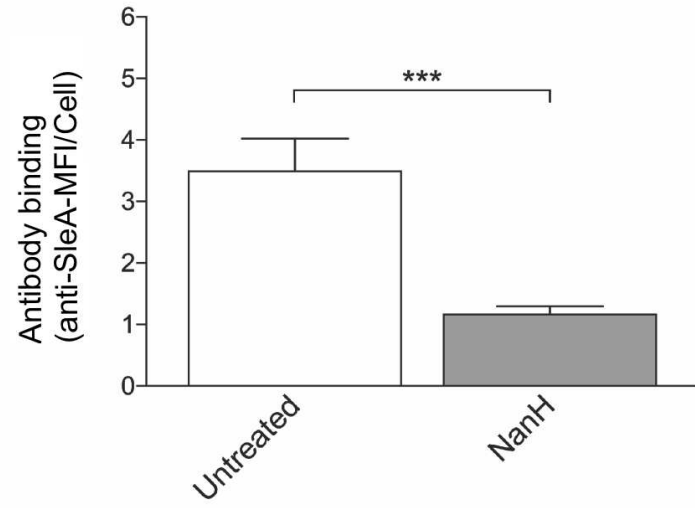
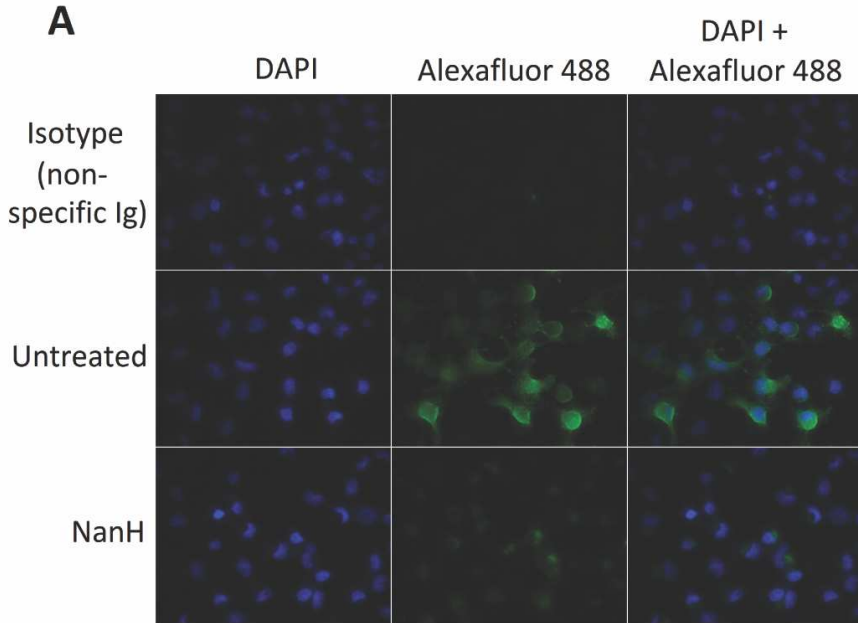


**D**

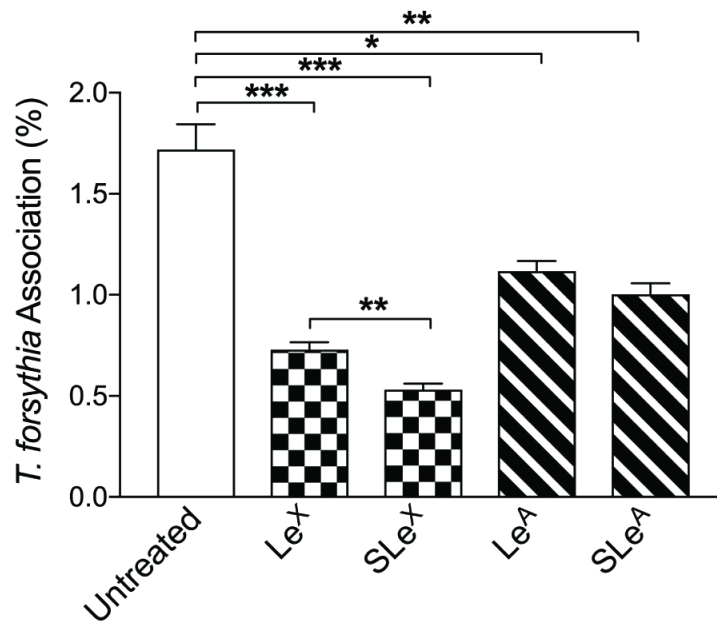
Substrate	$K_d$ ( $\mu\text{M}$ )
3-SL	$334 \pm 30$
6-SL	$528 \pm 23$
Lactose	$518 \pm 55$
SLe <sup>A</sup>	$178 \pm 11$
SLe <sup>X</sup>	$91 \pm 10$
Le <sup>A</sup>	$189 \pm 13$
Le <sup>X</sup>	$202 \pm 10$

# NanH-YMAP

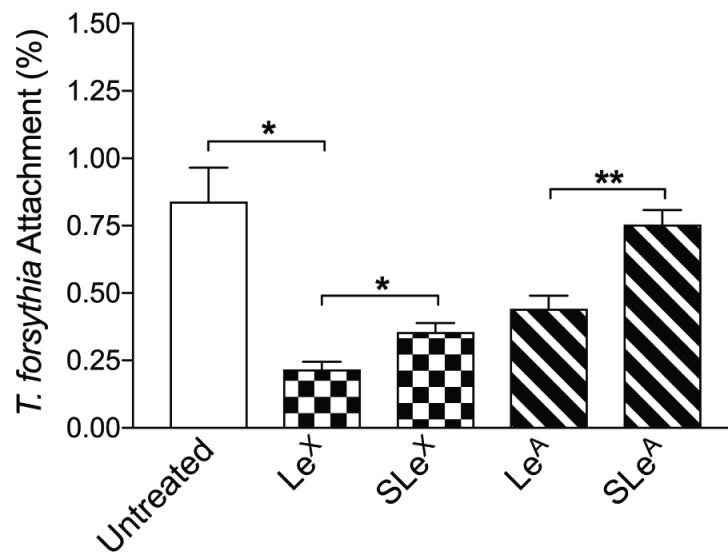




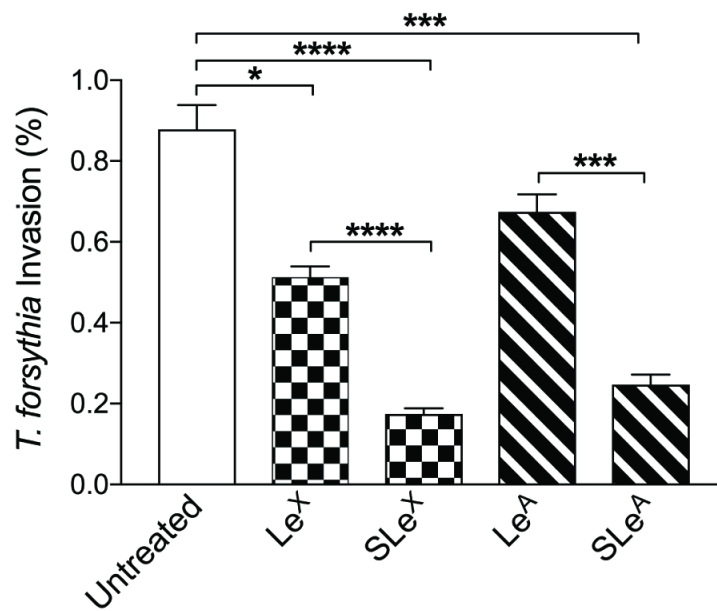
### A Total Association



### B Attachment



### C Invasion





	1	10	20	30	40	50	60
TF_92.A2	MKKFFWIIGLFAASMQMTRADSVYVQNPQIPILVDRTDNVLFRIIPDATKGDVLRNRLTI						
TF_43037	MKRFFLIIVGLLASMQMTRADSVYVQNPQIPILIIDRTDNVLFRISSIPDATKGDVLRNRLTI						
consensus>50	MKkFFLI!GLLASMQMTRADSVYVQNPQIPIL!DRTDNVLFRIrIPDATKGDVLRNRLTI						
	70	80	90	100	110	120	
TF_92.A2	RFGNEDKLSEVKAVRLFYAGTEAATKGRSRFAPVTYVSSHNI RNTRS ANP SYS I RQDEV T						
TF_43037	RFGNEDKLSEVKAVRLFYAGTEAATKGRSRFAPVTYVSSHNI RNTRS ANP SYS V RQDEV T						
consensus>50	RFGNEDKLSEVKAVRLFYAGTEAATKGRSRFAPVTYVSSHNI RNTRS ANP SYS ! RQDEV T						
	130	140	150	160	170	180	
TF_92.A2	TVANTLTLKTRQPMVKGINYFWVSVEMDRNTSLLSKLTSSTVTEVVINDKPAVIAGEQAAV						
TF_43037	TVANTLTLKTRQPMVKGINYFWVSVEMDRNTSLLSKLTPPTVTEAVINDKPAVIAGEQAAV						
consensus>50	TVANTLTLKTRQPMVKGINYFWVSVEMDRNTSLLSKLTPpTVTEvVINDKPAVIAGEQAAV						
	190	200	210	220	230	240	
TF_92.A2	RRMGIGVRHAGDDGSASFRIPGLVTTNKG TLLGVYDVRYNNSVDLQEHIDVGLSRSTDKG						
TF_43037	RRMGIGVRHAGDDGSASFRIPGLVTTNKG TLLGVYDVRYNNSVDLQEHVDVGLSRSTDKG						
consensus>50	RRMGIGVRHAGDDGSASFRIPGLVTTNKG TLLGVYDVRYNNSVDLQEH!DVGLSRSTDKG						
	250	260	270	280	290	300	
TF_92.A2	QTWEPMRIAMSFGETDGLPSGQNGVGDPSILVDERTNTVWVVAAWTHGMGNARAWTNSMP						
TF_43037	QTWEPMRIAMSFGETDGLPSGQNGVGDPSILVDERTNTVWVVAAWTHGMGNARAWTNSMP						
consensus>50	QTWEPMRIAMSFGETDGLPSGQNGVGDPSILVDERTNTVWVVAAWTHGMGNARAWTNSMP						
	310	320	330	340	350	360	
TF_92.A2	GMTPDETAQLMMVKSTDDGRTWSESTNITSQVKDPSWCFL LQGPGRGITMRDGT L VFPIQ						
TF_43037	GMTPDETAQLMMVKSTDDGRTWSEPTNITSQVKDPSWCFL LQGPGRGITMRDGT L VFPIQ						
consensus>50	GMTPDETAQLMMVKSTDDGRTWSEpTNITSQVKDPSWCFL LQGPGRGITMRDGT L VFPIQ						
	370	380	390	400	410	420	
TF_92.A2	FIDSLRVPHAGIMYSKDRGETWHIHQPARTNTTEAQVAEVEPGV LMLNMRDNRGGSRAVS						
TF_43037	FIDSLRVPHAGIMYSKDRGETWHIHQPARTNTTEAQVAEVEPGV LMLNMRDNRGGSRAVS						
consensus>50	FIDSLRVPHAGIMYSKDRGETWHIHQPARTNTTEAQVAEVEPGV LMLNMRDNRGGSRAVS						
	430	440	450	460	470	480	
TF_92.A2	ITRDLGKSWTEHSSNRSALPESICMASLISVKAKDNIIGKDLLLFSNPNTTEGRHHITIK						
TF_43037	ITRDLGKSWTEHSSNRSALPESICMASLISVKAKDNIIGKDLLLFSNPNTTEGRHHITIK						
consensus>50	ITRDLGKSWTEHSSNRSALPESICMASLISVKAKDNIIGKDLLLFSNPNTTEGRHHITIK						
	490	500	510	520	530		
TF_92.A2	ASLDGGVTWLP AHQVLLDEEDGWGYSCLSMIDRET V GIFYESSVAHMTFQAVKIKDLIR						
TF_43037	ASLDGGVTWLP AHQVLLDEEDGWGYSCLSMIDRET V GIFYESSVAHMTFQAVKIKDLIR						
consensus>50	ASLDGGVTWLP AHQVLLDEEDGWGYSCLSMIDRET V GIFYESSVAHMTFQAVKIKDLIR						

**Mw Marker**

(kDa)

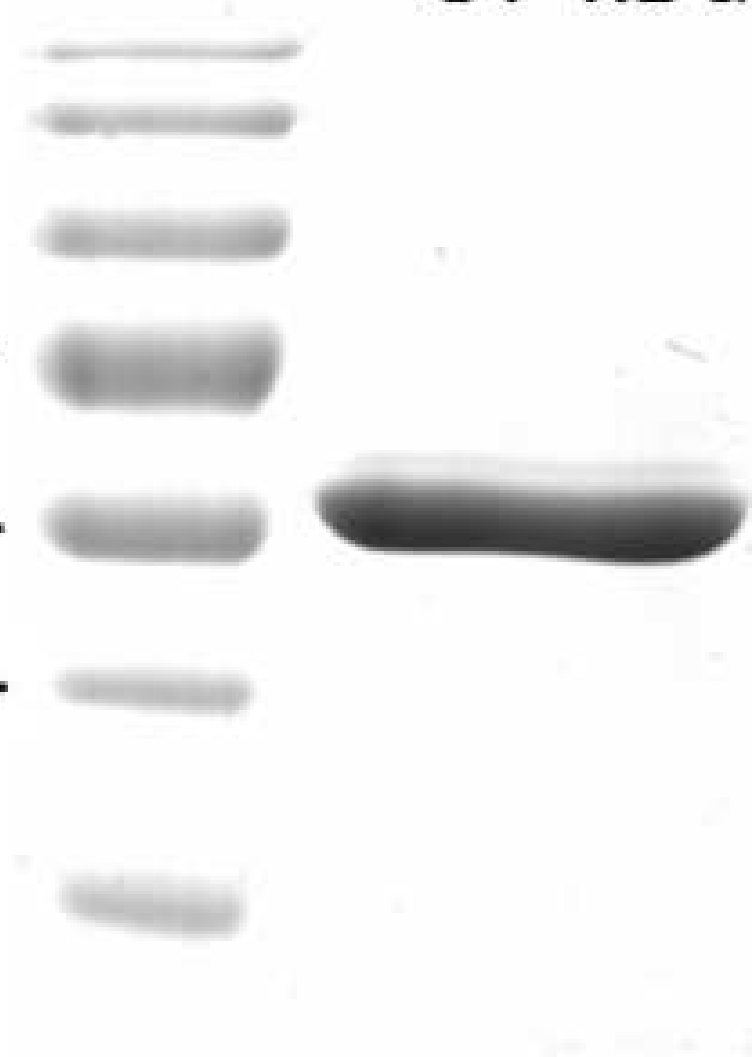
72-

55-

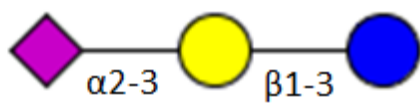
43-

**NanH**

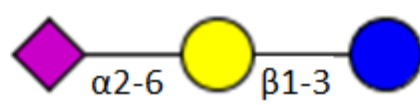
~57 kDa



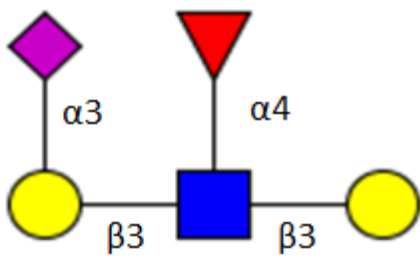
**3-SL**



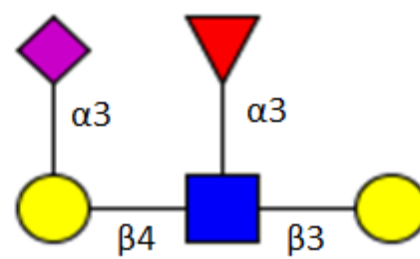
**6-SL**



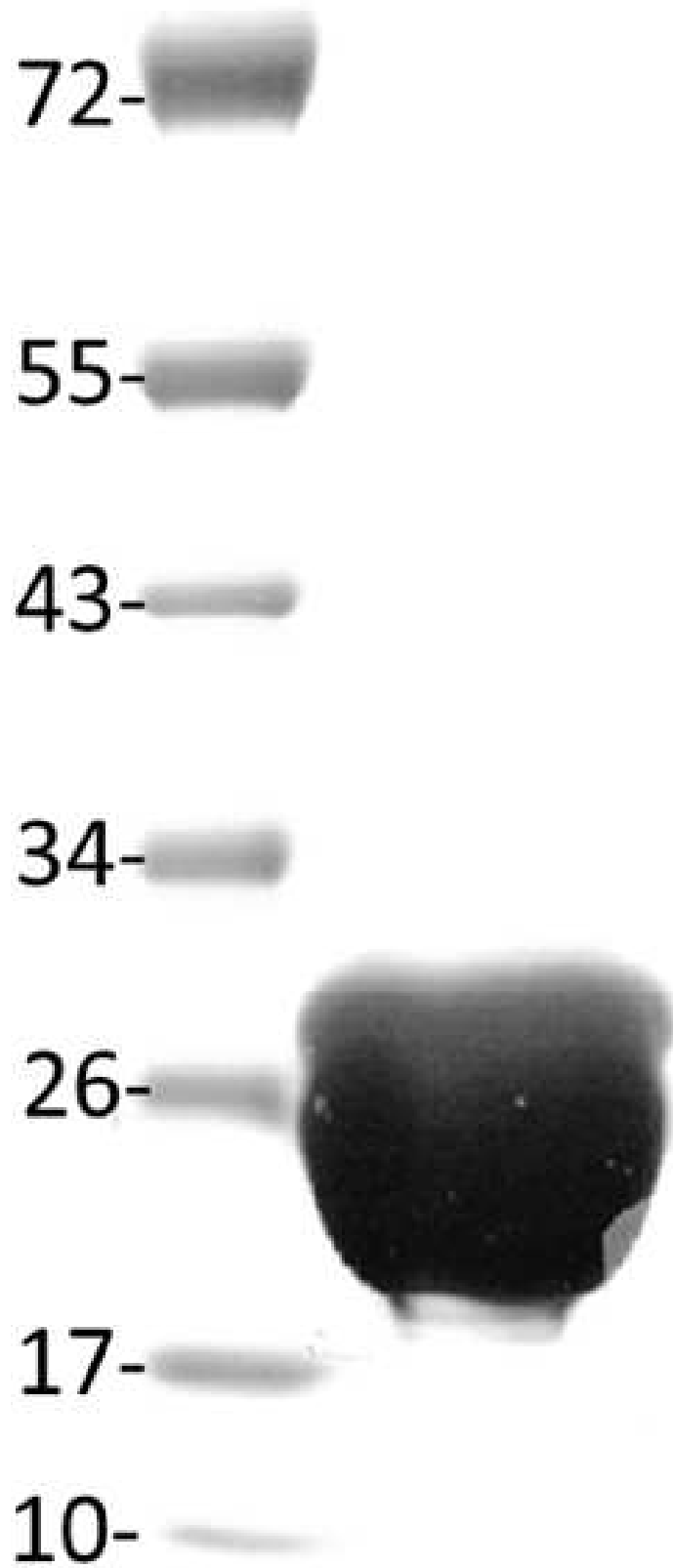
**SLe<sup>A</sup>**

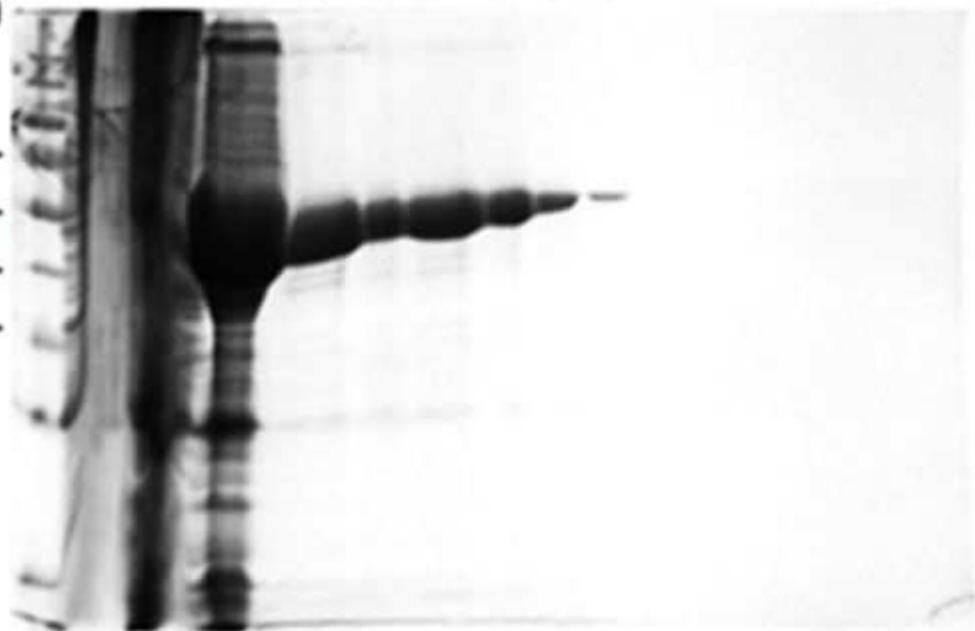


**SLe<sup>X</sup>**

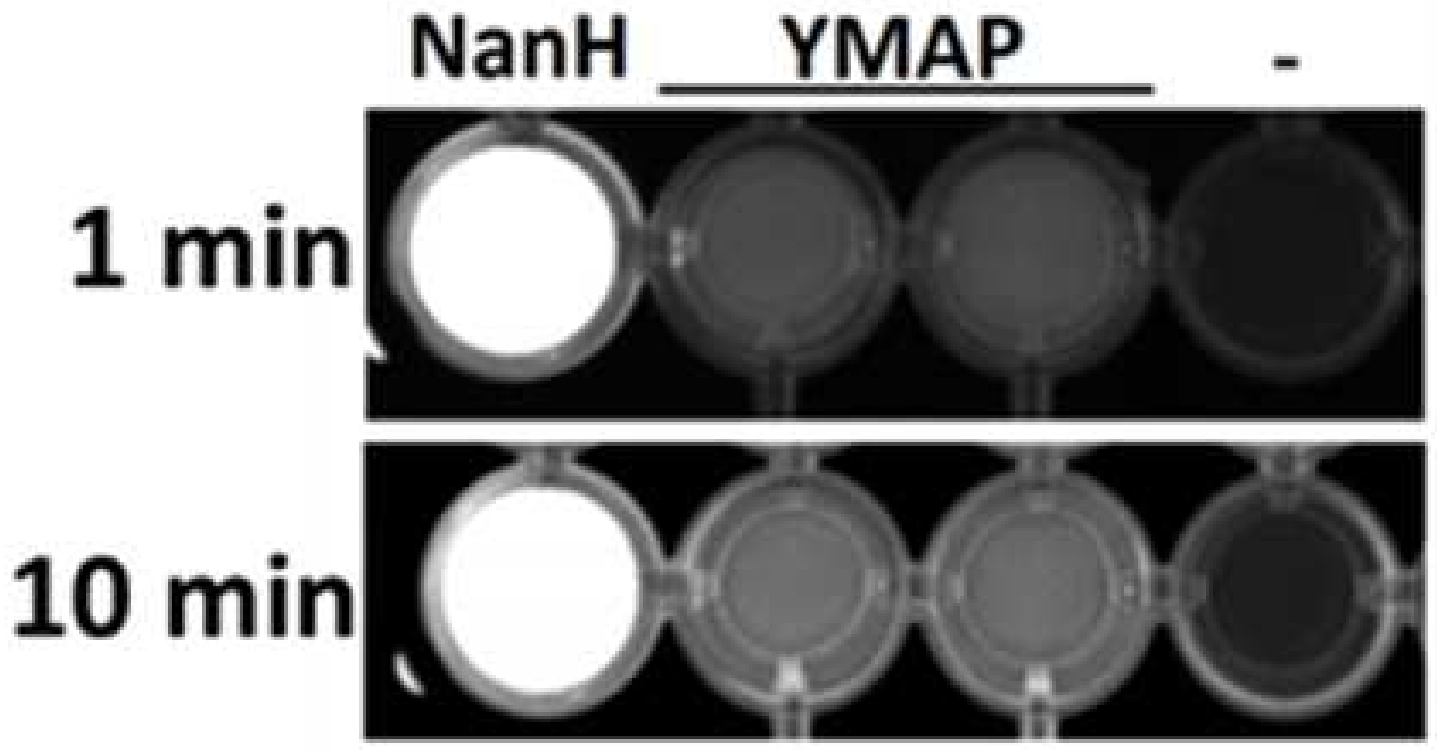


**Mw**      **NanH-**  
**Marker**   **CBM**  
(kDa)      ~18 kDa



**A****Eluted Fractions****Mw**  
**(kDa)****L Ins F W 1 2 3 4 5 6****72-**  
**55-**  
**43-**  
**34-**

**B**



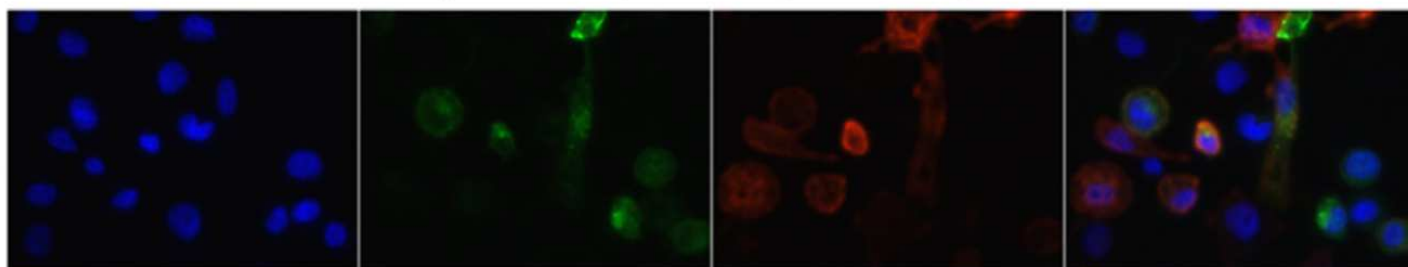
DAPI  
(nuclear stain)

FITC  
(SNA,  $\alpha$ 2-6 )

Texas Red  
(MAA,  $\alpha$ 2-3 )

Composite

Control  
(untreated)

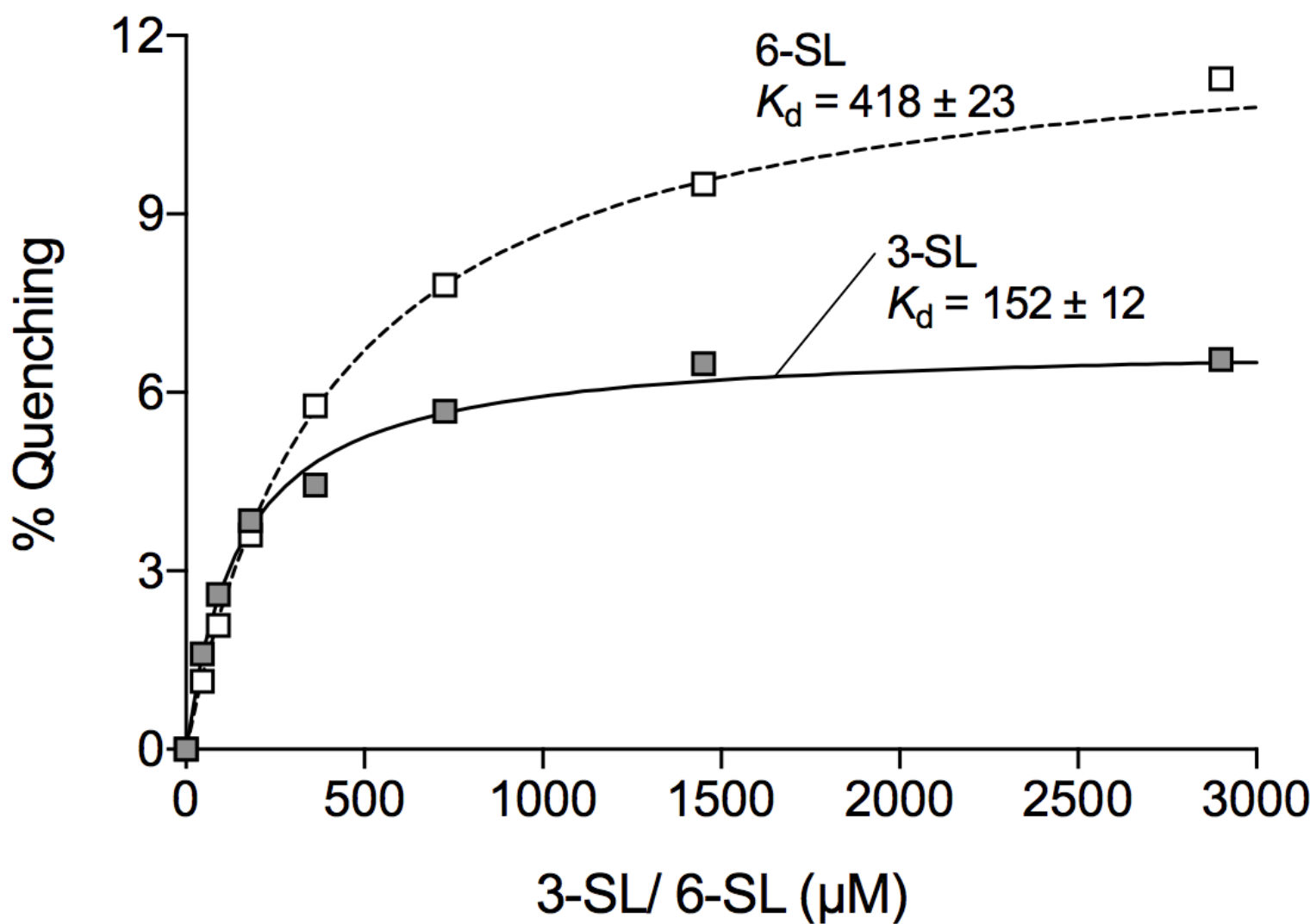


+50nM  
rNanH



Fig. S8

WT-NanH



## Tables

Site of Infection	Organism	Sialidase	Linkages Targeted	Linkage Preference	Reference
Respiratory tract	<b>Streptococcus pneumoniae</b>	NanA	$\alpha$ 2-3, $\alpha$ 2-6	$\alpha$ 2-6	[57]
		NanB	$\alpha$ 2-3	$\alpha$ 2-3	[57]
		NanC	$\alpha$ 2-3	$\alpha$ 2-3	[58]
	<b>Pseudomonas aeruginosa</b>	PAO1 neuraminidase	$\alpha$ 2-3, $\alpha$ 2-6	unknown	[59]
	<b>Pasturella multocida</b>	NanB	( $\alpha$ 2-3), $\alpha$ 2-6	$\alpha$ 2-6	[60]
		NanH	$\alpha$ 2-3, ( $\alpha$ 2-6)	$\alpha$ 2-3	[60]
<b>Corynebacterium diphtheriae</b>	NanH	$\alpha$ 2-3, $\alpha$ 2-6	$\alpha$ 2-6	[61]	
Gastrointestinal tract	<b>Clostridium perfringens</b>	NanI	$\alpha$ 2-3, $\alpha$ 2-6	$\alpha$ 2-3	[62]
		NanJ	$\alpha$ 2-3, $\alpha$ 2-6	$\alpha$ 2-6	[62]
		NanH	$\alpha$ 2-3, $\alpha$ 2-6	$\alpha$ 2-3	[62]
	<b>Salmonella Typhimurium</b>	NanH	$\alpha$ 2-3, $\alpha$ 2-6	$\alpha$ 2-3	[63]
	<b>Bacteroides thetaiotaomicron</b>	VPI-5482	$\alpha$ 2-3, $\alpha$ 2-6	$\alpha$ 2-6	[64]
	<b>Ruminococcus gnavus</b>	NanH	$\alpha$ 2-3	$\alpha$ 2-3	[65]
Oral cavity	<b>Porphyromonas gingivalis</b>	SiaPG	$\alpha$ 2-3, $\alpha$ 2-6	unknown	[12]
	<b>Treponema denticola</b>	TDE0471	$\alpha$ 2-3, $\alpha$ 2-6	unknown	[13]
	<b>Tannerella forsythia</b>	NanH	$\alpha$ 2-3, $\alpha$ 2-6	$\alpha$ 2-3	This study, [17]
	<b>Streptococcus oralis</b>	NanA	$\alpha$ 2-3, $\alpha$ 2-6	$\alpha$ 2-3	[66]
	<b>Streptococcus mitis</b> <sup>^</sup>	NanA*	$\alpha$ 2-3, $\alpha$ 2-6*	unknown	[67]

**Table 1. Sialic acid-linkage preferences of sialidases from bacteria associated with different mucosal sites.** Blue = Respiratory Tract, Green = GI tract, Pink = Oral Cavity. *P. multocida* is a respiratory pathogen of cattle, and can cause wound infections in humans. \*Not all *S. mitis* isolates possess sialidase activity, and the ability to target both sialic acid linkages is unknown, but presumably both  $\alpha$ 2-3 and  $\alpha$ 2-6 linkages can be targeted, as inferred by its homology with NanA from other Streptococci.